



**HAL**  
open science

# Force per cross-sectional area from molecules to muscles: a general property of biological motors

Jean-Pierre Rospars, Nicole Meyer-Vernet

## ► To cite this version:

Jean-Pierre Rospars, Nicole Meyer-Vernet. Force per cross-sectional area from molecules to muscles: a general property of biological motors. Royal Society Open Science, 2016, 3 (7), pp.UNSP 160313. 10.1098/rsos.160313 . hal-01390578

**HAL Id: hal-01390578**

**<https://hal.sorbonne-universite.fr/hal-01390578>**

Submitted on 2 Nov 2016

**HAL** is a multi-disciplinary open access archive for the deposit and dissemination of scientific research documents, whether they are published or not. The documents may come from teaching and research institutions in France or abroad, or from public or private research centers.

L'archive ouverte pluridisciplinaire **HAL**, est destinée au dépôt et à la diffusion de documents scientifiques de niveau recherche, publiés ou non, émanant des établissements d'enseignement et de recherche français ou étrangers, des laboratoires publics ou privés.



Distributed under a Creative Commons Attribution 4.0 International License



**Cite this article:** Rospars J-P, Meyer-Vernet N. 2016 Force per cross-sectional area from molecules to muscles: a general property of biological motors. *R. Soc. open sci.* **3**: 160313. <http://dx.doi.org/10.1098/rsos.160313>

Received: 7 May 2016

Accepted: 17 June 2016

**Subject Category:**

Biology (whole organism)

**Subject Areas:**

biomechanics/physiology/evolution

**Keywords:**

biological motors, specific tension, molecular motors, myofibrils, muscles

**Author for correspondence:**

Jean-Pierre Rospars

e-mail: [jean-pierre.rospars@versailles.inra.fr](mailto:jean-pierre.rospars@versailles.inra.fr)


Electronic supplementary material is available at <http://dx.doi.org/10.1098/rsos.160313> or via <http://rsos.royalsocietypublishing.org>.

# Force per cross-sectional area from molecules to muscles: a general property of biological motors

Jean-Pierre Rospars<sup>1</sup> and Nicole Meyer-Vernet<sup>2</sup>

<sup>1</sup>Institut National de la Recherche Agronomique (INRA), Unité Mixte de Recherche 1392 Institut d'Ecologie et des Sciences de l'Environnement de Paris, 78000 Versailles, France

<sup>2</sup>LESIA, Observatoire de Paris, CNRS, PSL Research University, UPMC, Sorbonne University, Paris Diderot, Sorbonne Paris Cité, 92195 Cedex Meudon, France

 JPR, 0000-0003-0797-5153

We propose to formally extend the notion of specific tension, i.e. force per cross-sectional area—classically used for muscles, to quantify forces in molecular motors exerting various biological functions. In doing so, we review and compare the maximum tensions exerted by about 265 biological motors operated by about 150 species of different taxonomic groups. The motors considered range from single molecules and motile appendages of microorganisms to whole muscles of large animals. We show that specific tensions exerted by molecular and non-molecular motors follow similar statistical distributions, with in particular, similar medians and (logarithmic) means. Over the  $10^{19}$  mass ( $M$ ) range of the cell or body from which the motors are extracted, their specific tensions vary as  $M^\alpha$  with  $\alpha$  not significantly different from zero. The typical specific tension found in most motors is about 200 kPa, which generalizes to individual molecular motors and microorganisms a classical property of macroscopic muscles. We propose a basic order-of-magnitude interpretation of this result.

## 1. Background

Living organisms use biological motors for various functions, which range from internal transport of ions and molecules in cells to motion of microorganisms and animals, the latter being driven by muscles. The forces developed by muscles are generally expressed as force per cross-sectional area, called specific tension or stress. It has been known for a long time that the vertebrate striated muscles can exert maximum tensions at constant length (isometric tension) of about 200–300 kPa which are on first

approximation independent of the muscle and the body mass [1]. This rule was extended to arthropod muscles with values in the range 300–700 kPa [2], although in some mollusc muscles stresses up to 1400 kPa were reported [3]. Later, a review of the literature based on muscles of 72 species of different taxonomic groups, including mammals, birds, reptiles, amphibians, molluscs, insects and crustaceans [4] concluded that there was no significant relationship between body mass and isometric tension, although isometric tension was found to be significantly higher in molluscs, crustaceans and amphibians than in other groups.

In the last 20 years, investigations were extended at the subcellular and molecular levels to investigate myofibrils (e.g. [5]), and non-muscular motors (e.g. [6]). The latter included measurement of forces developed by rotary or linear motors operating the  $F_0F_1$ -ATPase ion pump (e.g. [7,8]), bacterial flagella (e.g. [9]), bacterial pili (e.g. [10,11]), and the helical spasmoneme spring of the protozoan *Vorticella* (e.g. [12]). Investigations also included forces generated by single molecules producing tension used for locomotion or for other functions. The former include myosin II—a major component of myofibrils driving skeletal muscles (e.g. [13]), and axonemal dynein—bending flagella of eukaryotic cells (e.g. [14]). The latter include conventional kinesin (e.g. [15]), cytoplasmic dynein—transporting various cargos in cells (e.g. [16]), and RNA polymerase—moving along DNA while carrying transcription [17].

Despite their diversity, all these motors are based on protein machines generating forces. Macroscopic muscles are based on the myosin motor, whereas microorganisms and cells use other types of molecular motors. For comparing motors of so many different sizes, the convenient parameter is not the force  $F$ , which varies from several  $10^{-12}$  N for the myosin globular motor of cross-sectional area  $A \sim 40 \text{ nm}^2$  to approximately 500 N for a large muscle of cross section approximately  $20 \text{ cm}^2$ , but, as we intend to show, the specific tension  $F/A$  (all symbols and abbreviations are defined in table 1). In muscles, the approximate conservation of  $F/A$  between animals is an extension of a rule dating back to Galileo, that the strength of a structure is proportional to its cross section. Now, it turns out from the above numbers that the tension of the myosin molecular motor is of the same order of magnitude as the tension of macroscopic muscles (all references to tension here and elsewhere refer to specific tension unless otherwise noted). We will show that this property is not a coincidence but stems from the basic arrangement of cross-bridges in striated muscles. Furthermore, because biological molecular motors are based on protein machines that convert chemical energy into mechanical energy in similar ways (with the possible exception of pili and jump muscles), their tensions are expected to be of the same order of magnitude as that of myosin. Therefore, we propose to extend to molecular motors the concept of tension of macroscopic muscles and to compare their applied forces per unit cross-sectional area. That the forces per unit cross-sectional area may be similar for molecular motors and muscles agrees with results by Marden & Allen [18] and Marden [19], who show in a class of motors that maximum force output scales as the two-thirds power of motor's mass, close to the motor's cross-sectional area.

In order to make a meaningful comparison, we need to consider a representative set of muscle tensions, as well as the tension of the myosin motor and those of various other molecular motors. So, we analysed 329 published values of maximum forces or tension for approximately 265 diverse biological motors. These motors include single molecules, molecular assemblies, muscle cells and whole muscles with various functional demands. They come from free-living cells and multicellular organisms of diverse phyla spanning more than 18 orders of magnitude in mass from  $10^{-16}$  to  $10^3$  kg. Our primary interest was for motors involved in whole body motion, whereas the other motors were kept for comparison.

The three main questions we addressed on this basis are as follows. Can the notion of specific tension of muscles (force per cross-sectional area) be formally extended to propulsion of organelles and to individual molecular motors? How does this tension compare with that in muscles, and can the results be understood in terms of the basic structures of both molecular motors and muscle fibres? How does tension in motors devoted to cell or body motion compare with tension in other motors?

## 2. Material and methods

### 2.1. Motor forces

The main variable of interest in this paper is the force generated by molecules, molecular assemblies, muscle fibres and muscles. Our dataset includes 13 motor types aggregated in five motor classes depending on the nature of the generated force.

**Table 1.** List of abbreviations

<i>A</i>	cross-sectional area of motors
<i>F</i>	force exerted by motors
<i>V</i>	volume of molecular motors
Al	algae
Am	amphibian
Ar	arachnids
Ba	bacteria
Bi	birds
Cr	crustaceans
DA	axonemal dynein
DC	cytoplasmic dynein
Ec	echinoderms
<i>f</i>	specific tension of motors
FA	$F_0/F_1$ ATPase
Fl	muscular fibre
Fi	fishes
FL	flagellum
Fly	fly locomotors
Fu	fungi
In	insects
IQR	interquartile range
KI	kinesin
<i>m</i>	mass of molecular motors
<i>M</i>	mass of organisms
M1	single molecule
M2	molecular assembly
Ma	mammals
MF	myofibril
Mo	molluscs
MU	muscle <i>in vitro</i>
MV	muscle <i>in vivo</i>
MY	myosin
non-loc	non-locomotory
PI	pili
Pr	protozoa
Re	reptiles
RN	RNA polymerase
SP	spasmoneme
Swim	swim locomotors
Terr	terrestrial locomotors

(i) Forces generated by single molecules (denoted M1): myosin II, kinesin I, axonemal and cytoplasmic dynein, and RNA polymerase (other classes of myosin and kinesin were not considered because of insufficient data);

- (ii) forces produced by large molecular assemblies (denoted M2):  $F_0F_1$ -ATPase, bacterial flagella, pili, spasmonemes and myofibrils. These motors can be also classified as non-locomotory (ATPase) and locomotory (the others) or as rotary (ATPase, bacterial flagella) and linear (the others);
- (iii) forces produced by single muscle fibres (i. e. muscle cells) or bundles of a few muscle fibres (both denoted FI), frequently demembranated (skinned), while maximally stimulated and clamped at constant length (isometric contraction), with electrical or chemical stimulations;
- (iv) maximum force produced by dissected large bundles of fibres or isolated whole muscles stimulated isometrically with electrical stimulation of the nerve or the muscle (denoted MU); and
- (v) forces measured in behaving animals engaged in a wide range of activities including running, jumping, swimming and biting (denoted MV).

Single molecules (M1) and molecular assemblies (M2) are collectively called here 'molecular motors'. The other motors, muscle fibres (FI) and whole muscles (MU and MV) are called 'non-molecular motors'.

## 2.2. Identification of study reports

Values of forces generated by molecular and non-molecular motors were taken from 173 articles published in peer-reviewed journals for a wide variety of cells and animals. We sought a sample that is representative of the widest range of sizes and design varieties for as many species as possible (approx. 150 species were found) representing several different taxonomic groups, including bacteria, protozoa, algae, fungi, echinoderms, insects, crustaceans, molluscs, fishes, amphibian, reptiles, birds and mammals.

For molecular motors, we searched for articles providing the main variables of interest (either force for linear motors or torque and lever arm for rotary motors) for the 10 types listed above. Other types were not considered. For example, of the 14 classes of kinesin, only the most studied kinesin I was included and in the myosin superfamily which consists of at least 18 classes of motor proteins involved in a large variety of physiological processes, only class II myosin (conventional) responsible for muscle contraction was included; the other classes involved in phagocytosis, cell motility and vesicle transport were excluded. For each type, potentially relevant papers were searched using the Google Scholar database using as keywords the motor type plus 'force', 'torque' or 'pN'.

For non-molecular motors, we proceeded in two steps. First, relevant papers were identified from previous review papers [1,2,4,18]; all their cited references were included, except the rare cases for which the full text was not available or the paper could not be feasibly translated into English. Second, other potentially relevant papers were searched without restriction on language or date in the Google Scholar database using keywords ('specific tension', 'muscle stress', 'fibre', 'fiber', ' $\text{N}/\text{m}^2$ ', ' $\text{N m}^{-2}$ ', ' $\text{N}/\text{cm}^2$ ', ' $\text{N cm}^{-2}$ ', ' $\text{N mm}^{-2}$ ', 'pascal', 'kPa', 'physiological cross-sectional area', 'PCSA', 'CSA', etc.). Bibliographic searches were discontinued in April 2015.

The papers in this preliminary list were screened based on their title and abstract to exclude those unrelated to biological motors, then collected. The useful information was extracted from each of them (see below) with independent checks by the two authors for most of them. Papers without original measurements were excluded. Data published more than once by the same author(s) or reproduced by other authors were identified and only the paper with the original measurement was kept in the reference list. Measurements not fulfilling our criteria (stall force of single molecular motor, maximum isometric tension of non-molecular motors) were not considered. No relevant papers were excluded.

## 2.3. Motor tensions

For all motors, the measured forces  $F$  were normalized per cross-sectional area  $A$  (tension  $f = F/A$  expressed in Newton per square-metre or equivalently kilopascal).

For molecular motors the tensions were calculated from the published values (measured force or for rotary motors, torque and lever arm, tables 2 and 3) with the area  $A$  calculated from the volume  $V$  of the motor (with the order-of-magnitude approximation  $A = V^{2/3}$ , table 2), except for a few elongated shapes (pilus and spasmoneme) for which we estimated  $A$  from the diameter of the molecular assembly. For myosin,  $A$  was estimated from the head of the molecule.

For non-molecular motors the tensions ( $f = F/A$ ) were always given in the articles cited.

**Table 2.** Characteristic sizes of linear and rotary molecular motors. (Abb, abbreviation;  $m$ , motor mass (in kDa),  $m_{\text{pg}} = \alpha m_{\text{kDa}}$ , with  $\alpha = 10^{15}/N_A$  pg kDa $^{-1}$ ,  $N_A$ , Avogadro's number;  $V$ , motor volume (in nm $^3$ ),  $V = \alpha m_{\text{kDa}}/\rho$ , with  $\rho = 10^{-9}$  pg nm $^{-3}$ ;  $A$ , motor cross-section (in nm $^2$ ),  $A = V^{2/3}$ ;  $L$ , lever arm (in nm).)

type	motor	Abb	$m$ (kDa)	$V$ (nm $^3$ )	$A$ (nm $^2$ )	$L$ (nm)	reference
linear	RNA polymerase	RN	590	980	99	—	Mooney and Landick [20]
	dynein (motor part)	DA/DC	331	550	67	—	Reck-Peterson <i>et al.</i> [21], Carter <i>et al.</i> [22]
	kinesin	KI	120	199	34	—	Block [23]
	myosin	MY	130	216	36	—	Rayment <i>et al.</i> [24], Rayment & Holden [25], Goldman [26], Billington <i>et al.</i> [27]
rotary	bacterial $F_0$ ATP synthase	FA	180	299	45	3.5	Yoshida <i>et al.</i> [28], Hoffmann <i>et al.</i> [29]
	bacterial $F_1$ ATP synthase	FA	380	631	74	4.5	Yoshida <i>et al.</i> [28], Hoffmann <i>et al.</i> [29]
	bacterial flagellum	FL	$10^4$	$1.67 \times 10^4$	650	20	Berg [9], Reid <i>et al.</i> [30], Minamino <i>et al.</i> [31]

**Table 3.** Molecular motors. (No, line number; Ab, abbreviated motor name; Ty, motor type; M1 = single molecule, M2 = molecular assembly, including myofibrils and myocytes; U, organism: U = unicellular, Z = multicellular; C, S = swimming; T = terrestrial, solid surface; F = flying; N = non-locomotory; group, taxonomic group, see list of abbreviations; motor: m. = muscle; M, cell or body mass (kg); l, mass indicated in the cited article: Y = Yes, N = No; A, molecular area (nm<sup>2</sup>); F, force (pN) or torque (pN nm)/lever arm (nm) of rotary motors; f, specific tension (kPa); T, temperature (°C); R = room temperature; Comment, f. = force.)

no.	Ab	Ty	U	C	species	group	motor	M (kg)	l	A (nm <sup>2</sup> )	F (pN)	f (kPa)	T (°C)	comment	reference
<b>linear motors</b>															
1	RN	M1	U	N	<i>Escherichia coli</i>	Ba	RNA polymerase	$1.3 \times 10^{-15}$	N	99	25	253	—	stall force	Wang <i>et al.</i> [17]
2	DC	M1	U	N	<i>Saccharomyces cerevisiae</i> (yeast)	Fu	dynein (cytoplasmic)	$3 \times 10^{-13}$	N	67	7	104	25	stall force	Gennerich <i>et al.</i> [16]
3	DC	M1	Z	N	<i>Drosophila melanogaster</i> (fruit fly)	In	dynein (cytoplasmic, early embryo)	$0.9 \times 10^{-13}$	N	67	1.10	16	—	estimate per single dynein	Gross <i>et al.</i> [32]
4	DC	M1	Z	N	<i>Sus scrofa domestica</i> (pig)	Ma	dynein (cytoplasmic, brain)	$1.6 \times 10^{-13}$	N	67	7.50	112	25	active dynein stall force	Toba <i>et al.</i> [33]
5	DC	M1	Z	N	<i>Bos taurus</i> (bull)	Ma	dynein (cytoplasmic, brain)	$10^{-13}$	N	67	1.10	16	24	stall force	Mallik <i>et al.</i> [34]
6	DA	M1	Z	S	<i>Tetrahymena thermophile</i>	Pr	dynein (axonemal, cilia)	$3 \times 10^{-11}$	N	67	4.70	70	26	single molecule	Hirakawa <i>et al.</i> [35]
7	DA	M1	Z	S	<i>Chlamydomonas reinhardtii</i>	Al	dynein (axonemal, flagellum)	$5 \times 10^{-13}$	N	67	1.20	18	—	trap force	Sakakibara <i>et al.</i> [36]
8	DA	M1	U	S	<i>Hemientrotus pulcherimus</i>	Ec	dynein (axonemal, sperm)	$10^{-13}$	N	67	6	90	25	isolated arms	Shingyoji <i>et al.</i> [37]
9	DA	M1	U	S	<i>Bos taurus</i> (bull)	Ma	dynein (axonemal, flagellum-sperm)	$10^{-13}$	N	67	5	75	—	isometric stall force, indirect	Schmitz <i>et al.</i> [14] (M in Holcomb-Wygle <i>et al.</i> [38])
10	KI	M1	Z	N	<i>Loligo pealeii</i> (squid)	Mo	kinesin (optic lobe)	$10^{-12}$	N	34	5.50	162	R	stall force	Svoboda & Block [39]
11	KI	M1	Z	N	<i>Loligo pealeii</i> (squid)	Mo	kinesin	$10^{-12}$	N	34	6.50	191	—	maximum stall force	Visscher <i>et al.</i> [40], Schnitzer <i>et al.</i> [15]
12	KI	M1	Z	N	<i>Bos taurus</i> (cow)	Ma	kinesin (brain)	$10^{-11}$	N	34	6.70	197	26	uniform stall force	Higushi <i>et al.</i> [41]
13	KI	M1	Z	N	<i>Bos taurus</i> (cow)	Ma	kinesin (brain)	$10^{-11}$	N	34	4.50	132	30	near isometric	Hunt <i>et al.</i> [42]
14	KI	M1	Z	N	<i>Bos taurus</i> (cow)	Ma	kinesin (brain)	$10^{-11}$	N	34	5.40	159	25	force to stop single molecule	Meyhöfer & Howard [43]
15	KI	M1	Z	N	<i>Bos taurus</i> (cow)	Ma	kinesin (brain)	$10^{-11}$	N	34	7	206	26	stall force	Kojima <i>et al.</i> [44]
16	KI	M1	Z	N	<i>Homo sapiens</i> (man)	Ma	kinesin-1 (recombinant)	$10^{-11}$	N	34	7.60	224	—	single-kinesin maximum force	Jamison <i>et al.</i> [45]

(Continued.)

Table 3. (Continued.)

no.	Ab	Ty	U	C	species	group	motor	$M$ (kg)	$l$	$A$ (nm <sup>2</sup> )	$F$ (pN)	$F$ (kPa)	$T$ (°C)	comment	reference
17	MY	M1	Z	S	<i>Rana esculenta</i> (frog)	Am	myosin (tibialis anterior muscle)	$5 \times 10^{-8}$	N	36	3.60	100	4	isometric, indirect	Linari <i>et al.</i> [46]
18	MY	M1	Z	S	<i>Rana esculenta</i> (frog)	Am	Actomyosin (tibialis anterior m.)	$5 \times 10^{-8}$	N	36	10	278	4	indirect isometric (indep. n)	Piazzesi <i>et al.</i> [47]
19	MY	M1	Z	S	<i>Rana esculenta</i> (frog)	Am	myosin (tibialis anterior muscles)	$5 \times 10^{-8}$	N	36	5.70	158	4	indirect isometric (dep. on n)	Piazzesi <i>et al.</i> [48]
20	MY	M1	Z	T	<i>Oryctolagus cuniculus</i> (rabbit)	Ma	myosin (heavy meromyosin, ske. m.)	$5 \times 10^{-8}$	N	36	3.50	97	—	average isometric force	Finer <i>et al.</i> [49]
21	MY	M1	Z	T	<i>Oryctolagus cuniculus</i> (rabbit)	Ma	myosin (skeletal muscle)	$5 \times 10^{-8}$	N	36	5.70	158	27	peak isometric	Ishijima <i>et al.</i> [50]
22	MY	M1	Z	T	<i>Oryctolagus cuniculus</i> (rabbit)	Ma	myosin (heavy meromyosin, ske. m.)	$5 \times 10^{-8}$	N	36	3.30	92	R	direct (not isometric)	Miyata <i>et al.</i> [51]
23	MY	M1	Z	T	<i>Oryctolagus cuniculus</i> (rabbit)	Ma	myosin (psoas, fast skeletal m.)	$5 \times 10^{-8}$	N	36	6.30	175	32	indirect	Tsaturyan <i>et al.</i> [52]
24	MY	M1	Z	T	<i>Oryctolagus cuniculus</i> (rabbit)	Ma	myosin (skeletal white muscle)	$5 \times 10^{-8}$	N	36	6.50	181	R	direct (sliding not isometric)	Nishizaka <i>et al.</i> [53]
25	MY	M1	Z	T	<i>Oryctolagus cuniculus</i> (rabbit)	Ma	myosin (skeletal white muscle)	$5 \times 10^{-8}$	N	36	9.20	256	R	single molecule unbinding force	Nishizaka <i>et al.</i> [54]
26	MY	M1	Z	T	<i>Oryctolagus cuniculus</i> (rabbit)	Ma	Actomyosin (skeletal muscle)	$5 \times 10^{-8}$	N	36	9	250	—	direct isometric	Takagi <i>et al.</i> [55]
27	MY	M1	Z	T	<i>Oryctolagus cuniculus</i> (rabbit)	Ma	myosin (psoas)	$5 \times 10^{-8}$	N	36	6.30	175	32	indirect	
28	SP	M2	U	T	<i>Vorticella convallaria</i>	Pr	spasmoneme	$6.8 \times 10^{-11}$	N	$1.2 \times 10^6$	$4 \times 10^4$	33	—	maximum isometric tension	Moriyama <i>et al.</i> [56]
29	SP	M2	U	T	<i>Vorticella convallaria</i>	Pr	spasmoneme	$6.8 \times 10^{-11}$	N	$2.0 \times 10^6$	$7 \times 10^4$	35	—	not isometric tension	Upadhyaya <i>et al.</i> [12]
30	SP	M2	U	T	<i>Vorticella convallaria</i>	Pr	spasmoneme	$6.8 \times 10^{-11}$	N	$2.0 \times 10^6$	$2.5 \times 10^5$	125	—	isometric tension	Ryu <i>et al.</i> [57]
31	PI	M2	U	T	<i>Escherichia coli</i>	Ba	pili type P	$10^{-15}$	N	46	27	587	—	optical tweezers, unfolding f.	Jass <i>et al.</i> [58]

(Continued.)



Table 3. (Continued.)

no.	Ab	Ty	U	C	species	group	motor	M (kg)	J	A (nm <sup>2</sup> )	F (pN)	F (kPa)	T (°C)	comment	reference
32	PI	M2	U	T	<i>Escherichia coli</i>	Ba	pili type P	10 <sup>-15</sup>	N	46	27	587	—	optical tweezers	Fällman <i>et al.</i> [59]
33	PI	M2	U	T	<i>Escherichia coli</i>	Ba	pili type P	10 <sup>-15</sup>	N	46	28	609	—	isometric force	Andersson <i>et al.</i> [60]
34	PI	M2	U	T	<i>Escherichia coli</i>	Ba	pili type P	10 <sup>-15</sup>	N	46	35	761	—	atomic f. microscopy, plateau	Miller <i>et al.</i> [11]
35	PI	M2	U	T	<i>Escherichia coli</i>	Ba	pili type I	10 <sup>-15</sup>	N	48	60	1250	—	atomic force microscopy	Miller <i>et al.</i> [11]
36	PI	M2	U	T	<i>Neisseria gonorrhoeae</i>	Ba	pili type IV	10 <sup>-15</sup>	Y	36	70	1944	—	detachment force	Biais <i>et al.</i> [10] (M in kaiser [61], Meiz <i>et al.</i> [62])
rotary motors															
37	FA	M2	U	N	<i>Escherichia coli</i>	Ba	F0-ATPase (ionic pump)	1.3 × 10 <sup>-15</sup>	N	46	40/3.5	248	—		Noji <i>et al.</i> [63], Sambongi <i>et al.</i> [7]
38	FA	M2	U	N	<i>Bacillus</i>	Ba	F1ATPase	3 × 10 <sup>-15</sup>	N	74	40/4.5	120	23		Yasuda <i>et al.</i> [8]
39	FL	M2	U	S	<i>Escherichia coli</i>	Ba	flagellum (basal + hook)	1.6 × 10 <sup>-15</sup>	Y	650	4500/20	346	—	stall (or slow rotation)	Berry and Berg [64] (M in Berg [9,65])
40	FL	M2	U	S	<i>Vibrio alginolyticus</i>	Ba	flagellum	1.3 × 10 <sup>-15</sup>	N	650	2100/20	162	—	stall torque	Sowa <i>et al.</i> [66]
41	FL	M2	U	S	<i>Salmonella</i>	Ba	flagellum	4 × 10 <sup>-15</sup>	N	650	2100/20	162	23	torque at zero speed	Nakamura <i>et al.</i> [67]
42	FL	M2	U	S	<i>Streptococcus</i>	Ba	flagellum	2 × 10 <sup>-16</sup>	N	650	2500/20	192	22	torque at zero speed	Lowe <i>et al.</i> [68]
myofibrils															
43	MF	M2	Z	T	<i>Mus musculus</i> (mouse)	Ma	psoas (fast skeletal m.)	10 <sup>-11</sup>	N	—	—	91	20	single myofibril not stretched	Powers <i>et al.</i> [69]
44	MF	M2	Z	T	<i>Oryctolagus cuniculus</i> (rabbit)	Ma	psoas (fast skeletal m.)	5 × 10 <sup>-8</sup>	N	—	—	265	5	not skinned, single or few	Tesi <i>et al.</i> [5]
45	MF	M2	Z	T	<i>Oryctolagus cuniculus</i> (rabbit)	Ma	psoas (fast skeletal m.)	5 × 10 <sup>-8</sup>	N	—	—	186	10	bundle (1–3 myofibrils)	Telley <i>et al.</i> [70]
46	MF	M2	Z	T	<i>Oryctolagus cuniculus</i> (rabbit)	Ma	psoas (fast skeletal m.)	5 × 10 <sup>-8</sup>	N	—	—	250	23	single or 2–3 myofibrils	Shimamoto <i>et al.</i> [71]
47	MF	M2	Z	S	<i>Rana sp.</i> (frog)	Am	tibialis anterior & sartorius	5 × 10 <sup>-8</sup>	N	—	—	376	15	single myofibril	Colomo <i>et al.</i> [72]
48	MF	M2	Z	N	<i>Rana sp.</i> (frog)	Am	heart atrial myocyte	1.8 × 10 <sup>-12</sup>	N	—	—	149	15	single myocyte (1–5 myofibrils)	Colomo <i>et al.</i> [72] (M in Brandt <i>et al.</i> [73])

(Continued.)

Table 3. (Continued.)

no.	Ab	Ty	U	C	species	group	motor	$M$ (kg)	$l$	$A$ (nm <sup>2</sup> )	$F$ (pN)	$F$ (kPa)	$T$ (°C)	comment	reference
49	MF	M2	Z	N	<i>Rana esculenta</i> (frog)	Am	heart atrial	$1.8 \times 10^{-12}$	Y	—	—	120	20	single myocyte (1–5 myofibrils)	Brandt <i>et al.</i> [73]
50	MF	M2	Z	N	<i>Rana esculenta</i> (frog)	Am	heart ventricle	$3.5 \times 10^{-12}$	Y	—	—	124	20	single myocyte (1–5 myofibrils)	Brandt <i>et al.</i> [73]
51	MF	M2	Z	N	<i>Mus musculus</i> (mouse)	Ma	heart left ventricle	$10^{-11}$	N	—	—	119	10	bundle (2–6 myofibrils)	Kruger <i>et al.</i> [74]
52	MF	M2	Z	N	<i>Mus musculus</i> (mouse)	Ma	heart left ventricle	$10^{-11}$	N	—	—	138	10	bundle (2–6 myofibrils)	Stehle <i>et al.</i> [75]
53	MF	M2	Z	N	<i>Cavia porcellus</i> (guinea pig)	Ma	heart left ventricle	$10^{-11}$	N	—	—	161	10	bundle (2–6 myofibrils)	Stehle <i>et al.</i> [75]
54	MF	M2	Z	N	<i>Cavia porcellus</i> (guinea pig)	Ma	heart left ventricle	$10^{-11}$	N	—	—	149	10	bundle (2–6 myofibrils)	Stehle <i>et al.</i> [76]
55	MF	M2	Z	N	<i>Cavia porcellus</i> (guinea pig)	Ma	heart left ventricular trabeculae	$10^{-11}$	N	—	—	141	10	bundle (1–3 myofibrils)	Teley <i>et al.</i> [70]
56	MF	M2	Z	N	<i>Cavia porcellus</i> (guinea pig)	Ma	heart left ventricle	$10^{-11}$	N	—	—	196	10	bundle (2–6 myofibrils)	Stehle <i>et al.</i> [77]
57	MF	M2	Z	N	<i>Oryctolagus cuniculus</i> (rabbit)	Ma	heart right ventricle	$10^{-11}$	N	—	—	145	21	single myofibril	Linke <i>et al.</i> [78]
58	MF	M2	Z	N	<i>Homo sapiens</i> (human)	Ma	heart left ventricle	$10^{-11}$	N	—	—	151	10	bundle (2–6 myofibrils)	Stehle <i>et al.</i> [75]

All tensions were expressed in kilopascal. In papers giving several values or minimum and maximum, their mean was calculated. Values from different papers were never pooled. In tables 3 (molecular motors) and 4 (non-molecular motors) tensions given by different authors in different conditions for the same motor are listed separately (329 values). If the same motor of the same species, studied by different authors or the same authors in different conditions, are counted only once, the number of different motors is approximately 265 (the uncertainty arises from a few measurements in table 4 which were made on a mixture of distinct fibres or several muscles together).

## 2.4. Other motor classifications

The data were also analysed with respect to the structure of motors, their function and the taxonomic position of the organisms.

For comparing structures, the original 13 types, from molecules to muscles, were aggregated in five classes (M1, M2, FI, MU, MV) or two classes (molecular M1 + M2 and non-molecular) as defined above. In some figures and table 5, MF, for which the cross-section was indicated in the articles cited, was shown separately from the other M2 motors.

The functional groups were defined by the contribution of the motor to the overall movement of their parent organism, the four basic categories being swimming (Swim), flying (Fly), moving with respect to a solid surface (terrestrial Terr) and no direct contribution to locomotion (non-loc). Examples of non-loc motors are RNA polymerase, cytoplasmic dynein, kinesin,  $F_0/F_1$ -ATPase and various muscular motors (heart, diaphragm, wing closer, gill pump, claw closer, larynx, eye).

For taxonomic comparisons, groups 5 with number of  $f$  values less than 5 (protozoa, algae, fungi, echinoderms, arachnids) were excluded.

## 2.5. Body mass

Finally, the tensions were analysed with respect to the mass  $M$  of the 'body' that the motor contributes to move. For molecular motors this is the mass of the cell from which the motor was extracted. When not reported, cell masses were estimated from other sources or calculated from the cell size. In non-molecular motors, tensions were analysed with respect to the mass  $M$  of the corresponding animal. When not reported, body masses were also estimated from other sources. Note that as a consequence of these choices a different mass was used for a myosin molecule (molecular motor) and a muscle fibre (non-molecular motor) from the same organism. The organisms considered range in mass from the bacterium *Escherichia coli* ( $1.3 \times 10^{-15}$  kg) to the muscular fibre ( $5 \times 10^{-8}$  kg) for the cells, and from the mite *Archegozetes longisetosus* ( $10^{-7}$  kg) to the elephant (2500 kg) for the multicellular organisms.

For both  $f$  and  $M$ , means of a series of equivalent measurements by the same author(s) were preferred when available. When only minimum and maximum values were given, we took their mean.

## 2.6. Statistics

Statistical distributions were compared with the Kolmogorov–Smirnov test [194]. Multiple distributions were compared with the one-way analysis of variance (ANOVA) and corresponding multiple comparison of means using Tukey–Kramer adjustment. Slopes of least-square regressions of  $\log_{10}(f)$  versus  $\log_{10}(M)$  were compared with 0 using the  $F$  test. Details of statistical analyses are given as the electronic supplementary material, tables S1–S6 for ANOVA and multiple comparison of means and tables S7–S12 for regressions. All tests were performed with the MATLAB STATISTICAL TOOLBOX (The Mathworks, Natick, USA).

## 3. Results

The data have been analysed in terms of the maximum force per cross-sectional area  $f$ . We consider separately motors made of single molecules (denoted M1) and molecular assemblies (M2, MF) that we collectively call 'molecular motors', whereas the other motors, muscle fibres (FI) and whole muscles (MU for dissected muscles or MV for behaving animals) are called 'non-molecular motors'. We have also analysed the data in terms of the mass  $M$  of the 'body' that the motor contributes to move and to whether the motor contributes to the overall movement of the parent organism.

The characteristic sizes of molecular motors are given in the table 2. All data (species, taxonomic group, motor type, motor function, motor description, cell or body mass  $M$ , comment on  $M$ , specific

**Table 4.** Non-molecular motors. (Same columns as in table 3. I, mass indicated in the cited article: Y = yes, N = no, R = indicated as a range (mean is given). Motor: f, fibre, m, muscle, DDF deep digital flexor, EDL extensor digitorum longue, Gastr. gastrocnemius, SDF superficial digital flexor, VL vastus intermedius, VM vastus medialis. Comment: f, fibre, m, muscle.)

no.	Ty	C	species	group	motor	M (kg)	l	f (kPa)	T (°C)	comment	reference
1	Fl	F	<i>Drosophila melanogaster</i> (fruit fly)	In	indirect flight muscle	$1.9 \times 10^{-6}$	N	3.6	15	skinned f., active isometric	Wang <i>et al.</i> [79]
2	Fl	S	<i>Nephtrops norvegicus</i> (lobster)	Cr	superficial flexor m. 1st abdominal segment (slow S1)	0.50	N	105	22	skinned single f.	Holmes <i>et al.</i> [80]
3	Fl	S	<i>Nephtrops norvegicus</i> (lobster)	Cr	superficial flexor m. 1st abdominal segment (slow S2)	0.50	N	31	22	skinned single f.	Holmes <i>et al.</i> [80]
4	Fl	S	<i>Procambarus clarkii</i> (crayfish)	Cr	superficial abdominal extensor	0.05	N	430	20	not skinned single f.	Tameyasu [81]
5	Fl	F	<i>Bombus lucorum</i> + <i>B. terrestris</i> (bumblebee drone + worker)	In	dorsal longitudinal flight m. (asynchronous)	$5 \times 10^{-4}$	N	55	40	skinned single f.	Gilmour & Ellington [82]
6	Fl	S	<i>Carangus melampygus</i> (blue crevally, Pacific)	Fi	red f.	0.30	Y	43	25	skinned single f.	Johnston & Brill [83]
7	Fl	S	<i>Carangus melampygus</i> (blue crevally, Pacific)	Fi	white f.	0.30	Y	183	25	skinned single f.	Johnston & Brill [83]
8	Fl	S	<i>Chaenocephalus aceratus</i> (ice fish, Antarctic)	Fi	myotomal m. fast f., $-2 + 2^\circ$	1.03	Y	231	-1	skinned single f.	Johnston & Altringham [84]
9	Fl	S	<i>Eurhynchus affinis</i> (kawakawa, Pacific ocean)	Fi	red f.	3.20	Y	25	30	skinned single f.	Johnston & Brill [83]
10	Fl	S	<i>Eurhynchus affinis</i> (kawakawa, Pacific ocean)	Fi	white f.	3.20	Y	188	30	skinned single f.	Johnston & Brill [83]
11	Fl	S	<i>Gadus morhua</i> (North Sea cod, temperate)	Fi	myotomal m. fast f., $2-12^\circ$	84	Y	187	8	skinned single f.	Johnston & Altringham [84]
12	Fl	S	<i>Gadus morhua</i> (cod)	Fi	myotomal m. white f. (fast)	84	N	83	8	skinned single f.	Altringham & Johnston [85]
13	Fl	S	<i>Gadus morhua</i> (cod)	Fi	myotomal m. red f. (slow)	84	N	186	8	skinned 2-6 f.	Altringham & Johnston [85]

(Continued.)

Table 4. (Continued.)

no.	ly	C	species	group	motor	<i>M</i> (kg)	<i>l</i>	<i>f</i> (kPa)	<i>T</i> (°C)	comment	reference
14	FI	S	<i>Katsuwonus pelamis</i> (skipjack tuna, Pacific)	Fi	white f.	1.20	Y	157	25	skinned single f.	Johnston & Brill [83]
15	FI	S	<i>Katsuwonus pelamis</i> (skipjack tuna, Pacific)	Fi	red f.	1.20	Y	24	25	skinned single f.	Johnston & Brill [83]
16	FI	S	<i>Makaira nigricans</i> (Pacific blue marlin, tropical)	Fi	myotomal m. fast f., 10–30°	1.90	Y	156	20	skinned single f.	Johnston & Altringham [84]
17	FI	S	<i>Makaira nigricans</i> (Pacific Blue marlin)	Fi	white f.	85	R	176	25	skinned single f.	Johnston & Salamonski [86]
18	FI	S	<i>Makaira nigricans</i> (Pacific Blue marlin)	Fi	red f.	85	R	57	25	skinned 2–3 f.	Johnston & Salamonski [86]
19	FI	S	<i>Mugil cephalus</i> (grey mullet, Pacific reefs)	Fi	red f. (slow)	1.14	Y	52	20	skinned single f.	Johnston & Brill [83]
20	FI	S	<i>Mugil cephalus</i> (grey mullet, Pacific reefs)	Fi	white f.	1.14	Y	210	20	skinned single f.	Johnston & Brill [83]
21	FI	S	<i>Notothenia neglecta</i> (Antarctic fish)	Fi	white f. (fast)	0.60	Y	225	0	skinned single f.	Johnston & Brill [83]
22	FI	S	<i>Scorpaena notata</i> (Mediterranean fish)	Fi	anterior abdominal m. (fast f.)	0.023	Y	239	20	not skinned	Wakeling & Johnston [87]
23	FI	S	<i>Scyliorhinus canicula</i> (dogfish)	Fi	myotomal m. red f. (slow)	35	N	82	8	skinned 2–6 f.	Altringham & Johnston [85]
24	FI	S	<i>Scyliorhinus canicula</i> (dogfish)	Fi	myotomal m. white f. (fast)	35	N	183	8	skinned single f.	Altringham & Johnston [85]
25	FI	S	<i>Xenopus laevis</i> (clawed frog)	Am	iliofibularis m. (slow f.)	0.10	N	300	22	not skinned single f.	Lännergren [88,89] (in Medler [4])
26	FI	S	<i>Pseudemys scripta elegans</i> (freshwater terrapin)	Re	iliofibularis pale thick f. (fast glycolytic)	0.30	Y	183	15	skinned single f.	Mutungi & Johnston [90]
27	FI	S	<i>Pseudemys scripta elegans</i> (freshwater terrapin)	Re	iliofibularis medium thick f. (fast oxidative glycolytic)	0.30	Y	120	15	skinned single f.	Mutungi & Johnston [90]
28	FI	S	<i>Pseudemys scripta elegans</i> (freshwater terrapin)	Re	iliofibularis red thin (slow oxidative)	0.30	Y	71	15	skinned single f.	Mutungi & Johnston [90]

(Continued.)

Table 4. (Continued.).

no	ly	C	species	group	motor	M (kg)	f	f (kPa)	T (°C)	comment	reference
29	Fl	F	<i>Calypte anna</i> (hummingbird)	Bi	pectoralis	$4.7 \times 10^{-3}$	Y	12	20	single fibre	Reiser et al. [91]
30	Fl	F	<i>Calypte anna</i> (hummingbird)	Bi	ankle extensor	$4.7 \times 10^{-3}$	Y	94	20	single fibre	Reiser et al. [91]
31	Fl	F	<i>Gallus domesticus</i> (chicken white leghorn)	Bi	pectoralis major white or pale f.	1.50	N	165	15	skinned single f.	Reiser et al. [92]
32	Fl	N	<i>Gallus domesticus</i> (chicken white leghorn)	Bi	pectoralis major red strip ( $<1\%$ , fast f., wing closer)	1.50	N	174	15	skinned single f.	Reiser et al. [92]
33	Fl	F	<i>Gallus domesticus</i> (chicken white leghorn)	Bi	pectoralis major red strip (slow tonic f.)	1.50	N	126	15	skinned single f.	Reiser et al. [92]
34	Fl	F	<i>Gallus domesticus</i> (chicken white leghorn)	Bi	anterior latissimus dorsi (slow tonic f.)	1.50	N	75	15	skinned single f.	Reiser et al. [92]
35	Fl	F	<i>Taeniopygia guttata</i> (zebra finches)	Bi	pectoralis	$4.7 \times 10^{-3}$	Y	22	20	single fibre	Reiser et al. [91]
36	Fl	F	<i>Taeniopygia guttata</i> (zebra finches)	Bi	ankle extensor	$4.7 \times 10^{-3}$	Y	79	20	single fibre	Reiser et al. [91]
37	Fl	T	<i>Acinonyx jubatus</i> (cheetah)	Ma	gluteus, semitendinosus, longissimus m. (type 1)	41	Y	132	20	skinned fibre	West et al. [93]
38	Fl	T	<i>Acinonyx jubatus</i> (cheetah)	Ma	gluteus, semitendinosus, longissimus m. (type 2)	41	Y	195	20	skinned fibre	West et al. [93]
39	Fl	T	<i>Bos taurus</i> (cow Holstein)	Ma	usually soleus (slow f.)	160	Y	233	5.5	skinned single f.	Seow & Ford [94]
40	Fl	T	<i>Bos taurus</i> (cow Angus-Hereford)	Ma	~soleus (slow f.)	500	Y	60	5.5	skinned single f.	Seow & Ford [94]
41	Fl	T	<i>Bos taurus</i> (cow Holstein)	Ma	usually extensor digitorum longus (fast f.)	160	Y	248	5.5	skinned single f.	Seow & Ford [94]
42	Fl	T	<i>Bos taurus</i> (cow Angus-Hereford)	Ma	~extensor digitorum longus (fast f.)	500	Y	88	5.5	skinned single f.	Seow & Ford [94]
43	Fl	T	<i>Caracal caracal</i> (caracal)	Ma	vastus lateralis (type 2x)	15	N	211	12	single fibre	Kohn & Noakes [95]

(Continued.).

Table 4. (Continued.)

no	ty	C	species	group	motor	M (kg)	l	f (kPa)	T (°C)	comment	reference
44	Fl	T	<i>Equus caballus</i> (horse)	Ma	soleus (type 1, 23% of m.)	420	Y	84	15	skinned single f.	Rome <i>et al.</i> [96]
45	Fl	T	<i>Equus caballus</i> (horse)	Ma	soleus (type 2a, 43%)	420	Y	97	15	skinned single f.	Rome <i>et al.</i> [96]
46	Fl	T	<i>Equus caballus</i> (horse)	Ma	soleus (type 2b, 34%)	420	Y	120	15	skinned single f.	Rome <i>et al.</i> [96]
47	Fl	T	<i>Homo sapiens</i> (human cyclist)	Ma	vastus lateralis (type 1)	70	N	66	12	single fibre	Kohn & Noakes [95]
48	Fl	T	<i>Homo sapiens</i> (human cyclist)	Ma	vastus lateralis (type 2a)	70	N	113	12	single fibre	Kohn & Noakes [95]
49	Fl	T	<i>Homo sapiens</i> (human cyclist)	Ma	vastus lateralis (type 2ax)	70	N	155	12	single fibre	Kohn & Noakes [95]
50	Fl	T	<i>Homo sapiens</i> (human male 25–45 yr)	Ma	vastus lateralis (slow type 1)	70	N	44	12	skinned single f.	Bottinelli <i>et al.</i> [97]
51	Fl	T	<i>Homo sapiens</i> (human male 25–45 yr)	Ma	vastus lateralis (fast type 2)	70	N	61	12	skinned single f.	Bottinelli <i>et al.</i> [97]
52	Fl	T	<i>Homo sapiens</i> (human male & female)	Ma	quadriceps vastus lateralis and soleus (type 1)	65	N	210	15	skinned single f.	Larsson & Moss [98]
53	Fl	T	<i>Homo sapiens</i> (human male & female)	Ma	quadriceps vastus lateralis and soleus (type 2a fast)	65	N	200	15	skinned single f.	Larsson & Moss [98]
54	Fl	T	<i>Homo sapiens</i> (human male & female)	Ma	quadriceps vastus lateralis and soleus (type 2b fast)	65	N	190	15	freeze-dried single f.	Larsson & Moss [98]
55	Fl	T	<i>Macaca mulatta</i> (rhesus monkey)	Ma	soleus (slow type 1)	4	Y	180	15	skinned single f.	Fitts <i>et al.</i> [99]
56	Fl	T	<i>Macaca mulatta</i> (rhesus monkey)	Ma	medial gastrocnemius (slow type 1)	4		180	15	skinned single f.	Fitts <i>et al.</i> [99]
57	Fl	T	<i>Macaca mulatta</i> (rhesus monkey)	Ma	medial gastrocnemius (fast type 2)	4	Y	184	15	skinned single f.	Fitts <i>et al.</i> [99]
58	Fl	T	<i>Mus musculus</i> (mouse CD1 male)	Ma	tibialis ant., gastrocnemius, soleus (fast f.)	0.04	R	70	12	skinned single f.	Pellegrino <i>et al.</i> [100]
59	Fl	T	<i>Mus musculus</i> (mouse CD1 male)	Ma	tibialis ant., gastrocnemius, soleus (slow f.)	0.04	R	62	12	skinned single f.	Pellegrino <i>et al.</i> [100]

(Continued.)

Table 4. (Continued.)

no	ly	C	species	group	motor	M (kg)	l	f (kPa)	T (°C)	comment	reference
60	Fl	T	<i>Mus musculus</i> (mouse CBA/J)	Ma	extensor digitorum longue (fast)	0.02	Y	153	5.5	skinned single f.	Seow & Ford [94]
61	Fl	T	<i>Mus musculus</i> (mouse CBA/J)	Ma	soleus (slow)	0.02	Y	213	5.5	skinned single f.	Seow & Ford [94]
62	Fl	T	<i>Oryctolagus cuniculus</i> (rabbit New Zealand male)	Ma	tibialis ant., gastr., soleus, EDL, VL, psoas (slow f.)	3.15	R	45	12	skinned single f.	Pellegrino <i>et al.</i> [100]
63	Fl	T	<i>Oryctolagus cuniculus</i> (rabbit New Zealand male)	Ma	tibialis ant., gastr., soleus, EDL, VL, psoas (fast f.)	3.15	R	55	12	skinned single f.	Pellegrino <i>et al.</i> [100]
64	Fl	T	<i>Oryctolagus cuniculus</i> (rabbit)	Ma	tibialis anterior (type 2a)	2.5	N	140	20	single f.	Sweeney <i>et al.</i> [101] in Schiaffino & Reggiani [102]
65	Fl	T	<i>Oryctolagus cuniculus</i> (rabbit)	Ma	tibialis anterior (type 2b)	2.5	N	152	20	single f.	Sweeney <i>et al.</i> [101] in Schiaffino & Reggiani [102]
66	Fl	T	<i>Oryctolagus cuniculus</i> (rabbit New Zealand white)	Ma	psoas (type 2b)	2.5	R	125	12	skinned single f.	Sweeney <i>et al.</i> [103]
67	Fl	T	<i>Oryctolagus cuniculus</i> (rabbit New Zealand white)	Ma	tibialis anterior (type 2b)	2.5	R	120	12	skinned single f.	Sweeney <i>et al.</i> [103]
68	Fl	T	<i>Oryctolagus cuniculus</i> (rabbit New Zealand white)	Ma	tibialis anterior (type 2a chronic stim)	2.5	R	100	12	skinned single f.	Sweeney <i>et al.</i> [103]
69	Fl	T	<i>Oryctolagus cuniculus</i> (rabbit New Zealand white)	Ma	vastus intermedius (type 2a)	2.5	R	109	12	skinned single f.	Sweeney <i>et al.</i> [103]
70	Fl	T	<i>Oryctolagus cuniculus</i> (rabbit New Zealand white)	Ma	soleus (type 1)	2.5	R	107	12	skinned single f.	Sweeney <i>et al.</i> [103]

(Continued.)



Table 4. (Continued.)

no	Ty	C	species	group	motor	<i>M</i> (kg)	<i>I</i>	<i>f</i> (kPa)	<i>T</i> (°C)	comment	reference
71	Fl	T	<i>Oryctolagus cuniculus</i> (rabbit New Zealand white male)	Ma	plantaris (slow)	2.5	N	251	15	skinned single f.	Greaser <i>et al.</i> [104]
72	Fl	T	<i>Oryctolagus cuniculus</i> (rabbit New Zealand white male)	Ma	plantaris (intermediate)	2.5	N	253	15	skinned single f.	Greaser <i>et al.</i> [104]
73	Fl	T	<i>Oryctolagus cuniculus</i> (rabbit New Zealand white male)	Ma	plantaris (fast)	2.5	N	249	15	skinned single f.	Greaser <i>et al.</i> [104]
74	Fl	T	<i>Oryctolagus cuniculus</i> (rabbit New Zealand white)	Ma	extensor digitorum longue (fast)	2	Y	123	5.5	skinned single f.	Seow & Ford [94]
75	Fl	T	<i>Oryctolagus cuniculus</i> (rabbit New Zealand white)	Ma	soleus (slow)	2	Y	147	5.5	skinned single f.	Seow & Ford [94]
76	Fl	N	<i>Oryctolagus cuniculus</i> (rabbit)	Ma	diaphragm	$5 \times 10^{-8}$	N	99	20	single fibre	Reiser <i>et al.</i> [91]
77	Fl	T	<i>Oryctolagus cuniculus</i> (rabbit)	Ma	psoas muscle (type 2x)	$5 \times 10^{-8}$	N	195	20	single fibre	Reiser <i>et al.</i> [91]
78	Fl	T	<i>Ovis aries</i> (sheep)	Ma	~extensor digitorum longue (fast)	55	Y	159	5.5	skinned single f.	Seow & Ford [94]
79	Fl	T	<i>Ovis aries</i> (sheep)	Ma	~soleus (slow)	55	Y	198	5.5	skinned single f.	Seow & Ford [94]
80	Fl	T	<i>Panthera leo</i> (lion)	Ma	vastus lateralis (type 1)	180	N	162	12	single fibre	Kohn & Noakes [95]
81	Fl	T	<i>Panthera leo</i> (lion)	Ma	vastus lateralis (type 2x)	180	N	191	12	single fibre	Kohn & Noakes [95]
82	Fl	T	<i>Rattus norvegicus</i> (rat Wistar male)	Ma	tibialis anterior, plantaris, soleus (hindlimb, type 1)	0.25	N	68	12	skinned single f.	Bottinelli <i>et al.</i> [105]
83	Fl	T	<i>Rattus norvegicus</i> (rat Wistar male)	Ma	tibialis anterior, plantaris, soleus (slow type 1)	0.35	R	68	12	skinned single f.	Pellegrino <i>et al.</i> [100]
84	Fl	T	<i>Rattus norvegicus</i> (rat Wistar male)	Ma	tibialis anterior, plantaris, soleus (hindlimb, type 2a)	0.25	N	111	12	skinned single f.	Bottinelli <i>et al.</i> [105]

(Continued.)

Table 4. (Continued.)

no	Ty	C	species	group	motor	M (kg)	I	f (kPa)	T (°C)	comment	reference
85	FI	T	<i>Rattus norvegicus</i> (rat Wistar male)	Ma	tibialis anterior, plantaris, soleus (hindlimb, type 2x)	0.25	N	95	12	skinned single f.	Bottinelli <i>et al.</i> [105]
86	FI	T	<i>Rattus norvegicus</i> (rat Wistar male)	Ma	tibialis anterior, plantaris, soleus (hindlimb, type 2b)	0.25	N	82	12	skinned single f.	Bottinelli <i>et al.</i> [105]
87	FI	T	<i>Rattus norvegicus</i> (rat Wistar male)	Ma	tibialis anterior, plantaris, soleus (fast type 2)	0.35	R	96	12	skinned single f.	Pellegrino <i>et al.</i> [100]
88	FI	T	<i>Rattus norvegicus</i> (rat Holtzman female)	Ma	soleus red (slow f.)	0.165	N	223	27	skinned 2–6 f.	Sexton & Gersten [106]
89	FI	T	<i>Rattus norvegicus</i> (rat Hotzman)	Ma	medial gastrocnemius (fast f.)	0.165	R	235	27	skinned 3–6 f.	Sexton [107]
90	FI	T	<i>Rattus norvegicus</i> (rat Hotzman)	Ma	tibialis anterior	0.165	R	140	27	skinned 3–6 f.	Sexton [107]
91	FI	T	<i>Rattus norvegicus</i> (rat Sprague-Dawley)	Ma	extensor digitorum longue (fast)	0.20	Y	123	5.5	skinned single f.	Seow & Ford [94]
92	FI	T	<i>Rattus norvegicus</i> (rat Sprague-Dawley)	Ma	soleus (slow)	0.20	Y	100	5.5	skinned single f.	Seow & Ford [94]
93	FI	N	<i>Rattus norvegicus</i> (rat Sprague-Dawley)	Ma	diaphragm (type 1)	0.20	N	78	—	skinned single f.	Eddinger & Moss [108] in Schiaffino & Reggiani [102]
94	FI	N	<i>Rattus norvegicus</i> (rat Sprague-Dawley)	Ma	diaphragm (type 2a)	0.20	N	102	—	skinned single f.	Eddinger & Moss [108] in Schiaffino & Reggiani [102]
95	FI	N	<i>Rattus norvegicus</i> (rat Sprague-Dawley)	Ma	diaphragm (type 2b)	0.20	N	130	—	skinned single f.	Eddinger & Moss [108] in Schiaffino & Reggiani [102]
96	FI	T	<i>Rattus norvegicus</i> (rat Sprague-Dawley male)	Ma	tibialis anterior (fast)	0.25	Y	123	20	single fibre	Reiser <i>et al.</i> [91]
97	FI	T	<i>Rattus norvegicus</i> (rat Sprague-Dawley male)	Ma	soleus (slow)	0.25	Y	122	20	single fibre	Reiser <i>et al.</i> [91]
muscles <i>in vitro</i> or dissociated											
98	MU	S	<i>Alloteuthis subulata</i> (squid)	Mo	mantle m., ventral	0.50	N	262	11	piece of mantle	Milligan <i>et al.</i> [109]
99	MU	S	<i>Argopecten irradians</i> (bay scallop)	Mo	anterior side striated adductor	0.03	Y	242	10	bundle	Olson & Marsh [110]

(Continued.)

Table 4. (Continued.)

no	Iy	C	species	group	motor	M (kg)	f	f (kPa)	T (°C)	comment	reference
100	MU	S	<i>Sepia officinalis</i> (cuttlefish)	Mo	mantle m., ventral	0.50	N	226	11	piece of mantle	Milligan <i>et al.</i> [109]
101	MU	N	<i>Carcinus maenas</i> (crab male)	Cr	flagellum abductor m. (continuous action)	0.035	R	56	15	whole m. nerve stim	Stokes & Josephson [111]
102	MU	N	<i>Carcinus maenas</i> (crab male)	Cr	scaphognathite levator (pump water across gills)	0.019	R	120	15	whole m. nerve stim	Stokes & Josephson [111]
103	MU	S	<i>Homarus americanus</i> (lobster)	Cr	abdominal extensor (fast)	0.75	R	82	12	bundle 6 f. K + caffeine	Jahromi & Atwood [112]
104	MU	S	<i>Homarus americanus</i> (lobster)	Cr	abdominal extensor (slow)	0.75	R	442	12	bundle 6 f. K + caffeine	Jahromi & Atwood [112]
105	MU	N	<i>Homarus americanus</i> (lobster)	Cr	claw closer m. (crusher)	0.05	N	200	14	whole m. K + caffeine	Einer & Campbell [113] (M in Medler [4])
106	MU	N	<i>Homarus americanus</i> (lobster)	Cr	claw closer m. (closer)	0.05	N	300	14	whole m. K + caffeine	Einer & Campbell [113] (M in Medler [4])
107	MU	F	<i>Bombus terrestris</i> (bumblebee male)	In	dorsoventral flight m. (asynchronous)	$2.5 \times 10^{-4}$	R	38	30	whole m.	Josephson & Ellington [114]
108	MU	F	<i>Cotinus mutabilis</i> (beetle)	In	flight metathoracic basalar (asynchron. wing depressor)	$1.4 \times 10^{-3}$	Y	19	40	whole m.	Josephson <i>et al.</i> [115]
109	MU	F	<i>Libellula pulchella</i> (dragonfly male & female)	In	flight m.	$5.9 \times 10^{-4}$	N	120	28	whole m.	Fitzhugh & Marden [116] (M in Marden [117])
110	MU	F	<i>Manduca sexta</i> (hawkmoth summer-flying)	In	large dorsal longitudinal flight m.	$1.6 \times 10^{-3}$	Y	70	30	whole m.	Marden [117]
111	MU	F	<i>Neonoecephalus robustus</i> (katydid male)	In	flight & stridulation, mesothoracic	$1.0 \times 10^{-4}$	N	48	35	whole m.	Josephson [118]
112	MU	F	<i>Neonoecephalus robustus</i> (katydid male)	In	flight, metathoracic	$1.0 \times 10^{-4}$	N	137	35	whole m.	Josephson [118]
113	MU	F	<i>Neonoecephalus triops</i> (katydid male)	In	flight & stridulation, mesothoracic	$1.0 \times 10^{-4}$	N	58	35	whole m.	Josephson [118]
114	MU	F	<i>Neonoecephalus triops</i> (katydid male)	In	flight, metathoracic	$1.0 \times 10^{-4}$	N	126	35	whole m.	Josephson [118]

(Continued.)

Table 4. (Continued.)

no	Ty	C	species	group	motor	$M$ (kg)	$f$ (kPa)	$T$ (°C)	comment	reference
115	MU	F	<i>Operophtera bruceata</i> (moth male winter-flying)	In	large dorsal longitudinal flight m.	$1.17 \times 10^{-5}$	Y	139	18	whole m. Marden [117]
116	MU	F	<i>Schistocerca americana</i> (locust)	In	flight metathoracic 2nd tergo-coxal (synchronous)	$5.0 \times 10^{-4}$	N	363	25	whole m. Malamud & Josephson [119]
117	MU	N	<i>Gyrinus carpio</i> (carp)	Fi	hyohyoideus white & red f.	0.15	N	115	20	bundle Granzier <i>et al.</i> [120]
118	MU	S	<i>Gyrinus carpio</i> (carp)	Fi	red f.	0.15	N	116	15	bundle ~100 f. nerve stim Rome & Sosnicki [121]
119	MU	S	<i>Myoxocephalis scorpius</i> (sculpin)	Fi	white f., anterior + posterior	0.20	R	195	12	bundle 6–100 f. James <i>et al.</i> [122]
120	MU	S	<i>Myoxocephalis scorpius</i> (sculpin)	Fi	myotomal m. (fast f.)	0.27	R	198	5	bundle 6–20 f. James <i>et al.</i> [122]
121	MU	S	<i>Myoxocephalis scorpius</i> (sculpin)	Fi	fast	0.28	R	190	5	fast start escape James <i>et al.</i> [122]
122	MU	S	<i>Notothenia coriiceps</i> (Antarctic cod)	Fi	myotomal m. (fast f.)	0.154	Y	185	0	bundle 5–12 f. Franklin & Johnston [123]
123	MU	S	<i>Scyliorhinus canicula</i> (dogfish)	Fi	white myotomal m.	0.45	R	241	12	bundle 1–10 f. Curtin & Woledge [124]
124	MU	T	<i>Scyliorhinus canicula</i> (dogfish)	Fi	white myotomal m.	0.47	N	295	11	bundle 11–14 f. Lou <i>et al.</i> [125]
125	MU	S	<i>Stenotomus chrysops</i> (scup)	Fi	red myotomal m.	0.14	Y	197	20	bundle Coughlin <i>et al.</i> [126]
126	MU	S	<i>Stenotomus chrysops</i> (scup)	Fi	pink myotomal m.	0.14	N	151	20	bundle Coughlin <i>et al.</i> [126]
127	MU	T	<i>Ambystoma tigrinum</i> <i>nebulosum</i> (salamander)	Am	extensor iliotibialis pars anterior leg	$8.62 \times 10^{-3}$	Y	339	20	whole m. Else & Bennet [127]
128	MU	T	<i>Bufo americanus</i> (toad)	Am	white iliofibularis	0.04	Y	260	35	Johnston & Gleeson [128] in Medler [4]
129	MU	T	<i>Bufo marinus</i> (cane toad)	Am	white iliofibularis	0.18	Y	260	30	Johnston & Gleeson [128] in Medler [4]
130	MU	T	<i>Bufo woodhousei</i> (toad)	Am	white iliofibularis	0.11	Y	260	30	Johnston & Gleeson [128] in Medler [4]

(Continued.)

Table 4. (Continued.)

no	Ty	C	species	group	motor	M (kg)	I	f (kPa)	T (°C)	comment	reference
131	MU	N	<i>Hyla chrysoscelis</i> (tree frog male diploid)	Am	tensor chodarium (laryngeal muscle, call production)	$1.0 \times 10^{-2}$	N	55	25	whole muscle	McLister <i>et al.</i> [129]
132	MU	T	<i>Hyla chrysoscelis</i> (tree frog male diploid)	Am	sartorius (leg)	$1.0 \times 10^{-2}$	N	252	25	whole muscle	McLister <i>et al.</i> [129]
133	MU	N	<i>Hyla cinera</i> (tree frog male)	Am	tensor chodarium	$1.0 \times 10^{-2}$	N	181	25	whole muscle	McLister <i>et al.</i> [129]
134	MU	T	<i>Hyla cinera</i> (tree frog male)	Am	sartorius	$1.0 \times 10^{-2}$	N	285	25	whole muscle	McLister <i>et al.</i> [129]
135	MU	N	<i>Hyla versicolor</i> (tree frog male tetraploid)	Am	tensor chodarium	$1.0 \times 10^{-2}$	N	94	25	whole muscle	McLister <i>et al.</i> [129]
136	MU	T	<i>Hyla versicolor</i> (tree frog male tetraploid)	Am	sartorius	$1.0 \times 10^{-2}$	N	241	25	whole muscle	McLister <i>et al.</i> [129]
137	MU	T	<i>Osteopilus septentrionalis</i> (Cuban tree frog)	Am	sartorius	0.013	Y	244	20	whole muscle	Peplowski & Marsh [130]
138	MU	T	<i>Rana catesbeiana</i> (north American bullfrog male)	Am	abductor indicus longus (forelimb)	0.376	Y	285	22	whole m. nerve stim	Peters & Aulmer [131]
139	MU	T	<i>Rana catesbeiana</i> (frog male)	Am	flexor carpi radialis (forelimb)	$3.76 \times 10^{-4}$	Y	156	22	whole m. nerve stim	Peters & Aulmer [131]
140	MU	T	<i>Rana catesbeiana</i> (frog male)	Am	extensor carpi radialis (forelimb)	$3.76 \times 10^{-4}$	Y	237	22	whole m. nerve stim	Peters & Aulmer [131]
141	MU	T	<i>Rana catesbeiana</i> (frog male)	Am	extensor carpi ulnaris (forelimb)	$3.76 \times 10^{-4}$	Y	176	22	whole m. nerve stim	Peters & Aulmer [131]
142	MU	T	<i>Rana catesbeiana</i> (frog female)	Am	abductor indicus longus (forelimb)	$4.29 \times 10^{-4}$	Y	359	22	whole m. nerve stim	Peters & Aulmer [131]
143	MU	T	<i>Rana catesbeiana</i> (frog female)	Am	flexor carpi radialis (forelimb)	$4.29 \times 10^{-4}$	Y	118	22	whole m. nerve stim	Peters & Aulmer [131]
144	MU	T	<i>Rana catesbeiana</i> (frog female)	Am	extensor carpi radialis (forelimb)	$4.29 \times 10^{-4}$	Y	285	22	whole m. nerve stim	Peters & Aulmer [131]
145	MU	T	<i>Rana catesbeiana</i> (frog female)	Am	extensor carpi ulnaris (forelimb)	$4.29 \times 10^{-4}$	Y	197	22	whole m. nerve stim	Peters & Aulmer [131]

(Continued.)

Table 4. (Continued.)

no	Ty	C	species	group	motor	M (kg)	f	f (kPa)	T (°C)	comment	reference
146	MU	T	<i>Rana esculenta</i> (frog)	Am	sartorius	0.03	N	217	0	whole muscle	Stienen <i>et al.</i> [132]
147	MU	T	<i>Rana pipiens</i> (leopard frog)	Am	semimembranosus	0.03	N	255	25	bundle ~100 f	Lutz & Rome [133]
148	MU	T	<i>Xenopus laevis</i> (African clawed frog)	Am	gastrocnemius (main locomotory muscle in frogs)	$9.8 \times 10^{-3}$	Y	200	25	cold acclimated isolated m.	Seebacher <i>et al.</i> [134]
149	MU	T	<i>Dipsosaurus dorsalis</i> (lizard, desert iguana)	Re	iliofibularis (fast-twitch glycolytic region)	0.02	R	214	40	bundle	Marsh [135]
150	MU	T	<i>Sceloporus occidentalis</i> (lizard)	Re	iliofibularis (fast glycolytic f.)	0.0137	Y	188	35	bundle	Marsh & Bennet [136]
151	MU	F	<i>Coturnix chinensis</i> (blue-breasted quail)	Bi	pectoralis m. (flight)	0.046	Y	131	40	bundle	Askew & Marsh [137]
152	MU	T	<i>Cavia porcellus</i> (guinea pig)	Ma	soleus	0.13	R	147	20	whole muscle	Asmussen & Marechal [138]
153	MU	T	<i>Dipodomys spectabilis</i> (kangaroo rat)	Ma	gastrocnemius, plantaris, soleus (ankle extensor group)	0.11	Y	200	—	whole m. nerve stim	Perry <i>et al.</i> [139]
154	MU	T	<i>Dipodomys spectabilis</i> (kangaroo rat)	Ma	gastrocnemius + plantaris (soleus = 2%)	0.11	Y	200	30	whole m. nerve stim	Blewener <i>et al.</i> [140] in Ettema [141]
155	MU	T	<i>Felis silvestris</i> (cat)	Ma	gastrocnemius (25% slow S.f.)	4	N	60	—	single m. unit	Burke & Isairis [142], figure 4
156	MU	T	<i>Felis silvestris</i> (cat)	Ma	gastrocnemius (20% fast fatigue resistant FR f.)	4	N	270	—	single m. unit	Burke & Isairis [142], figure 4
157	MU	T	<i>Felis silvestris</i> (cat)	Ma	gastrocnemius (55% fast fatigable FF.f.)	4	N	172	—	single m. unit	Burke & Isairis [142], figure 4
158	MU	F	<i>Murina leucogaster</i> (korean bat)	Ma	biceps brachii	$7.6 \times 10^{-3}$	—	155	25	—	Choi <i>et al.</i> [143] in Medler [4]
159	MU	T	<i>Mus musculus</i> (mouse NMRI)	Ma	soleus	0.035	R	148	20	whole muscle	Asmussen & Marechal [138]
160	MU	T	<i>Mus musculus</i> (mouse T29/Re male)	Ma	soleus	0.02	N	154	37	whole muscle	Rowe [144]
161	MU	T	<i>Mus musculus</i> (mouse T29/Re female)	Ma	soleus	0.02	N	211	37	whole muscle	Rowe [144]

(Continued.)

Table 4. (Continued.)

no	Ty	C	species	group	motor	M (kg)	f	f (kPa)	T (°C)	comment	reference
162	MU	N	<i>Mus musculus</i> (mouse albino female)	Ma	diaphragm	0.03	R	176	35	1 mm strip	Luff [145]
163	MU	N	<i>Mus musculus</i> (mouse albino female)	Ma	inferior rectus	0.03	R	102	35	whole muscle	Luff [145]
164	MU	T	<i>Mus musculus</i> (mouse albino female)	Ma	extensor digitorum longus	0.03	R	249	35	whole muscle	Luff [145]
165	MU	T	<i>Mus musculus</i> (mouse albino female)	Ma	soleus	0.03	R	211	35	whole muscle	Luff [145]
166	MU	T	<i>Mus musculus</i> (mouse Swiss female)	Ma	soleus (slow twitch m.)	0.02	N	212	21	bundle	Barclay <i>et al.</i> [146]
167	MU	T	<i>Mus musculus</i> (mouse Swiss female)	Ma	extensor digitorum longue EDL (fast)	0.02	N	180	21	bundle	Barclay <i>et al.</i> [146]
168	MU	T	<i>Mus musculus</i> (mouse female)	Ma	extensor digitorum longus (2a + 2b f)	0.026	Y	243	37	whole muscle	Askew & Marsh [147]
169	MU	T	<i>Mus musculus</i> (mouse female)	Ma	soleus (2a fast oxida glycolyt + 1 slow oxida)	0.026	Y	269	37	whole muscle	Askew & Marsh [147]
170	MU	T	<i>Notomys alexis</i> (hopping mouse)	Ma	gastrocnemius	0.03	Y	238	30	whole muscle	Ettema [141]
171	MU	N	<i>Oryctolagus cuniculus</i> (rabbit)	Ma	extraocular inferior oblique	2.80	Y	39	35	whole muscle	Asmussen <i>et al.</i> [148]
172	MU	T	<i>Rattus norvegicus</i> (rat male Fisher 344)	Ma	medial gastrocnemius (slow S.f.)	0.46	R	167	36	motor unit nerve stim	Kanda & Hashizume [149]
173	MU	T	<i>Rattus norvegicus</i> (rat male Fisher 344)	Ma	medial gastrocnemius (fast fatigue resistant FR f.)	0.46	R	214	36	motor unit nerve stim	Kanda & Hashizume [149]
174	MU	T	<i>Rattus norvegicus</i> (rat male Fisher 344)	Ma	medial gastrocnemius (fast fatigable FF f.)	0.46	R	251	36	motor unit nerve stim	Kanda & Hashizume [149]
175	MU	T	<i>Rattus norvegicus</i> (rat)	Ma	medial gastrocnemius	0.31	Y	209	30	whole muscle	Ettema [141]

(Continued.)

Table 4. (Continued.)

no	Ty	C	species	group	motor	M (kg)	f (kPa)	T (°C)	comment	reference
176	MU	T	<i>Rattus norvegicus</i> (rat Wistar female)	Ma	extensor digitorum longue (tetanic, normal)	0.28	Y 281	—	whole m. nerve stim	Close [150]
177	MU	T	<i>Rattus norvegicus</i> (rat Wistar female)	Ma	extensor digitorum longue (tetanic, normal)	0.25	Y 294	35	whole m. nerve stim	Bárány & Close [151]
178	MU	T	<i>Rattus norvegicus</i> (rat male)	Ma	extensor digitorum longue (fast twitch)	0.20	N 360	35	bundle	Ranatunga [152]
179	MU	T	<i>Rattus norvegicus</i> (rat Wistar female)	Ma	soleus (tetanic, normal)	0.275	Y 189	—	whole m. nerve stim	Close [150]
180	MU	T	<i>Rattus norvegicus</i> (rat Wistar female)	Ma	soleus (tetanic, normal, mean oper. I–II–III)	0.25	Y 206	35	whole m. nerve stim	Bárány & Close [151]
181	MU	T	<i>Rattus norvegicus</i> (rat)	Ma	soleus (slow)	0.20	N 223	35	strip	Ranatunga [152]
182	MU	T	<i>Rattus norvegicus</i> (white rat)	Ma	gastrocnemius, plantaris, soleus (ankle extensor group)	0.24	Y 206	37	whole m. nerve stim	Perry <i>et al.</i> [139]
183	MU	N	<i>Rattus norvegicus</i> (rat)	Ma	diaphragm	0.20	N 159	37	strip 5–11 mm + nerve st	Goffart & Ritchie [153]
184	MU	N	<i>Rattus norvegicus</i> (rat)	Ma	diaphragm	0.30	205	26		Johnson <i>et al.</i> [154] in Medler [4]
185	MU	T	<i>Rattus norvegicus</i> (rat Wistar)	Ma	soleus	0.25	R 168	20	whole muscle	Asmussen & Marechal [138]
186	MU	T	<i>Thylogale biliaridieri</i> (wallaby red-bellied pademelon)	Ma	gastrocnemius medial head	5.00	R 200	32	whole m. nerve stim	Morgan <i>et al.</i> [155] in Ettema [141]
muscles <i>in vivo</i>										
187	MV	N	<i>Callinectes sapidus</i> (blue crab)	Cr	claw closer (crusher)	0.165	R 638	10	crushing	Govind & Blundon [156]
188	MV	N	<i>Callinectes sapidus</i> (blue crab)	Cr	claw closer (cutter)	0.165	R 514	10	cutting	Govind & Blundon [156]

(Continued.)



Table 4. (Continued.)

no	Ty	C	species	group	motor	$M$ (kg)	$f$	$f$ (kPa)	$T$ (°C)	comment	reference
189	MV	N	<i>Cancer antennarius</i> (crab)	Cr	claw closer N	0.112	Y	866	11	biting	Taylor [157]
190	MV	N	<i>Cancer branneri</i> (crab)	Cr	claw closer N	0.030	Y	1031	11	biting	Taylor [157]
191	MV	N	<i>Cancer gracilis</i> (crab)	Cr	claw closer N	0.156	Y	525	11	biting	Taylor [157]
192	MV	N	<i>Cancer magister</i> (crab)	Cr	claw closer N	0.310	Y	756	11	biting	Taylor [157]
193	MV	N	<i>Cancer oregonensis</i> (crab)	Cr	claw closer N	0.014	Y	1007	11	biting	Taylor [157]
194	MV	N	<i>Cancer productus</i> (crab)	Cr	claw closer N	0.136	Y	792	11	biting	Taylor [157]
195	MV	N	<i>Menippe mercenaria</i> (stone crab)	Cr	claw closer (crusher chela)	0.25	N	740	30	squeezing	Blundon [158] ( $M$ in Medler [4])
196	MV	N	<i>Menippe mercenaria</i> (stone crab)	Cr	claw closer (cutter chela)	0.25	N	785	30	squeezing	Blundon [158] ( $M$ in Medler [4])
197	MV	N	<i>Archezogetes longisetosus</i> (mite)	Ar	claws	$1.0 \times 10^{-7}$	Y	1200	—	holding	Heethoff & Koerner [159]
198	MV	T	<i>Athous haemorrhoidalis</i> (click beetle)	In	M4 jumping m.	$40 \times 10^{-6}$	Y	700	>25	jumping	Evans [160]
199	MV	T	<i>Carabus problematicus</i> (click beetle)	In	femoral rotator m. (hind leg)	$0.35 \times 10^{-3}$	Y	210	23	pushing	Evans [161]
200	MV	N	<i>Cyclommatus metallifer</i> (stag beetle male)	In	mandible closer muscles	$1.36 \times 10^{-3}$	Y	180	22	biting	Goyens <i>et al.</i> [162]
201	MV	F	<i>Drosophila hydei</i> (fruit fly female)	In	flight m.	$1.90 \times 10^{-6}$	N	40	—	tethered flight	Dickinson & Lighton [163]
202	MV	T	<i>Schistocerca gregaria</i> (locust female)	In	extensor tibiae (metathoracic leg)	$3 \times 10^{-3}$	R	700	30	jumping	Bennet-Clark [164]
203	MV	T	<i>Spilopsyllus cuniculus</i> (rabbit flea)	In	metathoracic leg	$0.45 \times 10^{-6}$	Y	300	—	jumping	Bennet-Clark & Lucey [165]
204	MV	S	<i>Xenopus</i> (frog)	Am	plantaris longus	0.10	—	200	—	swimming	Richards unpublished in Biewener [166]
205	MV	T	<i>Anas platyrhynchos</i> (mallard duck)	Bi	lateral gastrocnemius m.	1.05	Y	126	40	walking	Biewener & Coming [167]

(Continued.)

Table 4. (Continued.)

no	Ty	C	species	group	motor	M (kg)	f (kPa)	T (°C)	comment	reference
206	MV	S	<i>Anas platyrhynchos</i> (mallard duck)	Bi	lateral gastrocnemius m.	1.05	Y 62	40	swimming	Biewener & Coming [167]
207	MV	F	<i>Anas platyrhynchos</i> (mallard duck)	Bi	pectoralis	1.0	Y 236	40	ascending flight	Williamson <i>et al.</i> [168]
208	MV	F	<i>Columba livia</i> (pigeon)	Bi	pectoralis (flight m.)	0.31	R 76	40	ascending flight	Dial & Biewener [169]
209	MV	T	<i>Numida meleagris</i> (guinea fowl)	Bi	digital flexor-IV (hind limb)	1.25	Y 115	—	jumping	Biewener [166]
210	MV	T	<i>Numida meleagris</i> (guinea fowl)	Bi	digital flexor-IV (hind limb)	1.25	Y 130	—	running	Daley & Biewener [170]
211	MV	T	<i>Numida meleagris</i> (guinea fowl)	Bi	lateral gastrocnemius (hind limb)	1.25	Y 133	—	Jumping	Biewener [166]
212	MV	T	<i>Numida meleagris</i> (guinea fowl)	Bi	lateral gastrocnemius (hind limb)	1.25	Y 39	—	running	Daley & Biewener [170]
213	MV	F	<i>Sturnus vulgaris</i> (starling)	Bi	pectoralis, oxidative f.	0.072	Y 122	40	level flight	Biewener <i>et al.</i> [171]
214	MV	T	<i>Canis familiaris</i> (dog)	Ma	gastrocnemius + plantaris (ankle extensors)	36	310	—	jumping	Alexander [172]
215	MV	T	<i>Canis familiaris</i> (dog)	Ma	biceps femoris + 4 others (hip extensors)	36	270	—	jumping	Alexander [172]
216	MV	T	<i>Canis familiaris</i> (dog)	Ma	rectus femoris + VM + VL (knee extensors)	36	240	—	jumping	Alexander [172]
217	MV	T	<i>Canis familiaris</i> (dog)	Ma	triceps surae (elbow extensor)	36	290	—	jumping	Alexander [172]
218	MV	T	<i>Canis familiaris</i> (dog)	Ma	gastrocnemius, plantaris	36	Y 340	37	galloping 15.5 m s <sup>-1</sup>	Jayes & Alexander [173]
219	MV	T	<i>Canis familiaris</i> (dog)	Ma	biceps femoris + 4 others	36	Y 150	37	galloping 15.5 m s <sup>-1</sup>	Jayes & Alexander [173]
220	MV	T	<i>Canis familiaris</i> (dog)	Ma	sartorius, rectus femoris, tensor fasciae latae	36	Y 310	37	galloping 15.5 m s <sup>-1</sup>	Jayes & Alexander [173]
221	MV	T	<i>Canis familiaris</i> (dog)	Ma	rhomboideus	36	Y 300	37	galloping 15.5 m s <sup>-1</sup>	Jayes & Alexander [173]
222	MV	T	<i>Canis familiaris</i> (dog)	Ma	latissimus dorsi	36	Y 380	37	galloping 15.5 m s <sup>-1</sup>	Jayes & Alexander [173]
223	MV	T	<i>Canis familiaris</i> (dog)	Ma	pectoralis profundus	36	Y 260	37	galloping 15.5 m s <sup>-1</sup>	Jayes & Alexander [173]

(Continued.)

Table 4. (Continued.)

no	Ty	C	species	group	motor	M (kg)	I	f (kPa)	T (°C)	comment	reference
224	MV	T	<i>Canis familiaris</i> (dog)	Ma	serratus ventralis thoracis	36	Y	300	37	galloping 15.5 m s <sup>-1</sup>	Jayes & Alexander [173]
225	MV	T	<i>Canis familiaris</i> (dog)	Ma	pectorales superficiales	36	Y	370	37	galloping 15.5 m s <sup>-1</sup>	Jayes & Alexander [173]
226	MV	T	<i>Capra hircus</i> (goat)	Ma	superficial digital flexor	34	Y	58	—	cantering	McGuigan <i>et al.</i> unpublished in Biewener [166]
227	MV	T	<i>Capra hircus</i> (goat)	Ma	gastrocnemius	34	Y	72	—	cantering	McGuigan <i>et al.</i> unpublished in Biewener [166]
228	MV	T	<i>Dipodomys spectabilis</i> (kangaroo rat)	Ma	gastrocnemius, plantaris, soleus (ankle extensor group)	0.11	Y	69	—	hopping 1.5 m s <sup>-1</sup>	Perry <i>et al.</i> [139]
229	MV	T	<i>Dipodomys spectabilis</i> (kangaroo rat)	Ma	ankle extensors	0.11	R	38	—	hopping slow 0.7 m s <sup>-1</sup>	Biewener <i>et al.</i> [140]
230	MV	T	<i>Dipodomys spectabilis</i> (kangaroo rat)	Ma	ankle extensors	0.11	R	105	—	hopping fast 1.9 m s <sup>-1</sup>	Biewener <i>et al.</i> [140]
231	MV	T	<i>Dipodomys spectabilis</i> (kangaroo rat)	Ma	triceps surae	0.11	Y	297	—	jumping peak force	Biewener & Blickhan [174] in Biewener [166]
232	MV	T	<i>Equus caballus</i> (horse)	Ma	fore DDF & fore SDF, gastrocnemius	275	Y	66	—	walking peak f	Biewener [175]
233	MV	T	<i>Equus caballus</i> (horse)	Ma	fore DDF & fore SDF, gastrocnemius	275	Y	107	—	trotting peak f	Biewener [175]
234	MV	T	<i>Equus caballus</i> (horse)	Ma	DDF, SDF, gastrocnemius	275	Y	157	—	galloping peak f	Biewener [175]
235	MV	T	<i>Equus caballus</i> (horse)	Ma	DDF, SDF, gastrocnemius	275	Y	240	—	highest stress	Biewener [175]
236	MV	T	<i>Felis silvestris</i> (cat)	Ma	plantaris, SDF	3.6	<	123	—	trotting	Biewener [166] based on Herzog <i>et al.</i> [176]
237	MV	T	<i>Felis silvestris</i> (cat)	Ma	gastrocnemius	3.6	<	73	—	trotting	Biewener [166] based on Herzog <i>et al.</i> [176]
238	MV	T	<i>Homo sapiens</i> (human)	Ma	triceps surae	76	Y	151	37	running 4 m s <sup>-1</sup>	Thorpe <i>et al.</i> [177]
239	MV	T	<i>Homo sapiens</i> (human)	Ma	quadriceps	76	Y	255	37	running 4 m s <sup>-1</sup>	Thorpe <i>et al.</i> [177]
240	MV	T	<i>Homo sapiens</i> (human)	Ma	hip extensors	76	Y	110	37	running 4 m s <sup>-1</sup>	Thorpe <i>et al.</i> [177]
241	MV	T	<i>Homo sapiens</i> (human)	Ma	triceps surae	76	Y	101	37	high jump	Thorpe <i>et al.</i> [177]
242	MV	T	<i>Homo sapiens</i> (human)	Ma	quadriceps	76	Y	277	37	high jump	Thorpe <i>et al.</i> [177]
243	MV	T	<i>Homo sapiens</i> (human)	Ma	hip extensors	76	Y	120	37	high jump	Thorpe <i>et al.</i> [177]
244	MV	T	<i>Homo sapiens</i> (human male & female)	Ma	quadriceps	69.5	Y	76	37	test chair before training	Rutherford & Jones [178]

(Continued.)

Table 4. (Continued.)

no	Ty	C	species	group	motor	<i>M</i> (kg)	<i>f</i> (kPa)	<i>T</i> (°C)	comment	reference
245	MV	T	<i>Homo sapiens</i> (human male & female)	Ma	quadriceps	69.5	Y 82	37	test chair after training	Rutherford & Jones [178]
246	MV	T	<i>Homo sapiens</i> (human elderly 67.1 ± 2 yr)	Ma	vastus lateralis (knee)	73.5	Y 236	37	control pre-training	Reeves <i>et al.</i> [179]
247	MV	T	<i>Homo sapiens</i> (human elderly 67.1 ± 2 yr)	Ma	vastus lateralis (knee)	73.5	Y 215	37	control post-training	Reeves <i>et al.</i> [179]
248	MV	T	<i>Homo sapiens</i> (human elderly 74.3 ± 3.5 yr)	Ma	vastus lateralis (knee)	69.7	Y 270	37	test pre-training	Reeves <i>et al.</i> [179]
249	MV	T	<i>Homo sapiens</i> (human elderly 74.3 ± 3.5 yr)	Ma	vastus lateralis (knee)	69.7	Y 321	37	test post-training	Reeves <i>et al.</i> [179]
250	MV	T	<i>Homo sapiens</i> (human men 28.2 ± 3.6 yr)	Ma	quadriceps	78.8	Y 550	37	isokinetic dynamometer	O'Brien <i>et al.</i> [180]
251	MV	T	<i>Homo sapiens</i> (human women 27.4 ± 4.2 yr)	Ma	quadriceps	64	Y 573	37	isokinetic dynamometer	O'Brien <i>et al.</i> [180]
252	MV	T	<i>Homo sapiens</i> (human boys 8.9 ± 0.7 yr)	Ma	quadriceps	35.6	Y 540	37	isokinetic dynamometer	O'Brien <i>et al.</i> [180]
253	MV	T	<i>Homo sapiens</i> (human girls 9.3 ± 0.8 yr)	Ma	quadriceps	41.9	Y 598	37	isokinetic dynamometer	O'Brien <i>et al.</i> [180]
254	MV	T	<i>Homo sapiens</i> (human men)	Ma	biceps femoris + 4 others (knee)	61.3	Y 53	37	isokinetic dynamometer	Kanehisa <i>et al.</i> [181]
255	MV	T	<i>Homo sapiens</i> (human men)	Ma	quadriceps femoris (knee extensors)	61.3	Y 79	37	isokinetic dynamometer	Kanehisa <i>et al.</i> [181]
256	MV	T	<i>Homo sapiens</i> (human women)	Ma	knee flexors	58.5	Y 39	37	isokinetic dynamometer	Kanehisa <i>et al.</i> [181]
257	MV	T	<i>Homo sapiens</i> (human women)	Ma	knee extensors	58.5	Y 63	37	isokinetic dynamometer	Kanehisa <i>et al.</i> [181]
258	MV	T	<i>Homo sapiens</i> (human men)	Ma	biceps brachii & brachialis (elbow flexors)	61.3	Y 132	37	isokinetic dynamometer	Kanehisa <i>et al.</i> [181]

(Continued.)

Table 4. (Continued.)

no	Ty	C	species	group	motor	M (kg)	f	f (kPa)	T (°C)	comment	reference
259	MV	T	<i>Homo sapiens</i> (human men)	Ma	triceps brachii (elbow extensors)	61.3	Y	111	37	isokinetic dynamometer	Kanehisa <i>et al.</i> [181]
260	MV	T	<i>Homo sapiens</i> (human women)	Ma	elbow flexors	58.5	Y	137	37	isokinetic dynamometer	Kanehisa <i>et al.</i> [181]
261	MV	T	<i>Homo sapiens</i> (human women)	Ma	elbow extensors	58.5	Y	110	37	isokinetic dynamometer	Kanehisa <i>et al.</i> [181]
262	MV	T	<i>Homo sapiens</i> (human men 28 ± 4 yr)	Ma	soleus	75	Y	150	37	isokinetic dynamometer	Maganaris <i>et al.</i> [182]
263	MV	T	<i>Homo sapiens</i> (human men 28 ± 4 yr)	Ma	tibialis anterior	75	Y	155	37	isokinetic dynamometer	Maganaris <i>et al.</i> [182]
264	MV	T	<i>Homo sapiens</i> (human males 34 ± 4.7 yr)	Ma	quadriceps vastus lateralis	74.1	Y	237	37	isometric voluntary contract.	Narici <i>et al.</i> [183]
265	MV	T	<i>Homo sapiens</i> (human males 34 ± 4.7 yr)	Ma	quadriceps vastus intermedius	74.1	Y	241	37	isometric volunt. contraction	Narici <i>et al.</i> [183]
266	MV	T	<i>Homo sapiens</i> (human males 34 ± 4.7 yr)	Ma	quadriceps vastus medialis	74.1	Y	279	37	isometric volunt. contraction	Narici <i>et al.</i> [183]
267	MV	T	<i>Homo sapiens</i> (human males 34 ± 4.7 yr)	Ma	quadriceps rectus femoris	74.1	Y	243	37	isometric volunt. contraction	Narici <i>et al.</i> [183]
268	MV	T	<i>Homo sapiens</i> (human males 38 ± 8 yr)	Ma	gastrocnemius medialis	67.8	Y	97	37	whole muscle + MRI	Narici <i>et al.</i> [183]
269	MV	T	<i>Homo sapiens</i> (human males 21.3 ± 3.4 yr)	Ma	quadriceps femoris	76.2	Y	297	37	max. volunt. contrac. (2 meth)	Erskine <i>et al.</i> [184]
270	MV	T	<i>Homo sapiens</i> (human young 22 yr)	Ma	triceps surae (ankle plantar flexor)	70		329	37	electrically evoked contract.	Davies <i>et al.</i> [185]
271	MV	T	<i>Homo sapiens</i> (human)	Ma	ankle plantar flexor	70	N	108	37	voluntary isometric torque	Fukunaga <i>et al.</i> [186]
272	MV	T	<i>Homo sapiens</i> (human)	Ma	ankle plantar flexor	70	N	382	37	external force	Haxton [187] in Maganaris <i>et al.</i> [182]
273	MV	T	<i>Homo sapiens</i> (human)	Ma	ankle plantar flexor	70	N	628	37	external force	Herman [188] in Maganaris <i>et al.</i> [182]
274	MV	T	<i>Homo sapiens</i> (human)	Ma	ankle plantar flexor	70	N	549	37	external force	Reys [189] in Maganaris <i>et al.</i> [182]
275	MV	T	<i>Homo sapiens</i> (human)	Ma	ankle plantar flexor	70	N	412	37	external force	Weber [190] in Maganaris <i>et al.</i> [182]

(Continued.)

Table 4. (Continued.)

no	Ty	C	species	group	motor	$M(\text{kg})$	$f$ (kPa)	$T$ (°C)	comment	reference
276	MV	T	<i>Loxodonta africana</i> (elephant)	Ma	knee quadriceps	2500	140	37	running 4–4.5 m s <sup>-1</sup>	Alexander <i>et al.</i> [191]
277	MV	T	<i>Loxodonta africana</i> (elephant)	Ma	ankle extensors	2500	140	37	running 4–4.5 m s <sup>-1</sup>	Alexander <i>et al.</i> [191]
278	MV	T	<i>Loxodonta africana</i> (elephant)	Ma	elbow triceps	2500	140	37	running 4–4.5 m s <sup>-1</sup>	Alexander <i>et al.</i> [191]
279	MV	T	<i>Macropus eugenii</i> (tamarin wallaby)	Ma	plantaris	4.8	262	—	hopping 5.5 m s <sup>-1</sup>	Biewener & Baudinette [192]
280	MV	T	<i>Macropus eugenii</i> (tamarin wallaby)	Ma	gastrocnemius	4.8	227	—	hopping 5. m s <sup>-1</sup>	Biewener & Baudinette [192]
281	MV	T	<i>Macropus rufogriseus</i> (rock wallaby)	Ma	triceps surae	6.6	279	—	jumping	McGowan & Biewener unpublished in Biewener [166]
282	MV	T	<i>Macropus rufogriseus</i> (rock wallaby)	Ma	triceps surae	6.6	201	—	hopping	McGowan & Biewener unpublished in Biewener [166]
283	MV	T	<i>Macropus rufus</i> (red kangaroo juvenile)	Ma	plantaris + gastrocnemius (ankle extensors)	24	R 300	—	hopping	Alexander & Vernon [193]
284	MV	T	<i>Macropus rufus</i> (red kangaroo juvenile)	Ma	hip extensors	24	R 190	—	hopping	Alexander & Vernon [193]
285	MV	T	<i>Macropus rufus</i> (red kangaroo juvenile)	Ma	rectus femoris + VL + VI + VM (knee extensors)	24	R 240	—	hopping	Alexander & Vernon [193]
286	MV	T	<i>Protemnodon rufogrisea</i> (Bennett's wallaby)	Ma	plantaris + gastrocnemius (ankle extensors)	10.5	Y 150	—	hopping	Alexander & Vernon [193]
287	MV	T	<i>Protemnodon rufogrisea</i> (Bennett's wallaby)	Ma	hip extensors	10.5	Y 140	—	hopping	Alexander & Vernon [193]
288	MV	T	<i>Protemnodon rufogrisea</i> (Bennett's wallaby)	Ma	rectus femoris + VL + VI + VM (knee extensors)	10.5	Y 75	—	hopping	Alexander & Vernon [193]
289	MV	T	<i>Rattus norvegicus</i> (white rat)	Ma	gastrocnemius, plantaris, soleus (ankle extensors)	0.24	Y 70	—	galloping 1.5 m s <sup>-1</sup>	Perry <i>et al.</i> [139]
290	MV	T	<i>Syncerus caffer</i> (buffalo)	Ma	ankle extensors	500	Y 150	37	galloping 5 m s <sup>-1</sup>	Alexander <i>et al.</i> [191]
291	MV	T	<i>Syncerus caffer</i> (buffalo)	Ma	elbow triceps	500	Y 300	37	galloping 5 m s <sup>-1</sup>	Alexander <i>et al.</i> [191]

**Table 5.** Summary statistics<sup>a</sup> of specific tension  $f$  (in kPa) Per main motor types and functions.

		$n$	min	max	Q10	Q90	med.	IQR	mean	s.d.
motor types	all	349	4	1944	62	354	174	136	212	196
	all molecular	58	16	1944	72	524	160	129	239	303
	all non-molecular	291	4	1200	62	339	180	137	206	167
	PI	6	587	1944	587	1875	685	663	956	547
	non-PI	343	4	1200	62	312	167	134	199	158
motor types (except PI)	molecular	52	16	376	60	254	155	86	156	77
	non-molecular	291	4	1200	62	339	180	137	206	167
	M1	27	16	278	28	252	158	102	146	75
	M2 <sup>b</sup>	9	33	346	34	307	162	107	158	99
	MF	16	91	376	119	264	149	60	173	71
	M2 + MF	25	33	376	91	265	149	70	167	80
	FI	97	4	430	53	230	123	105	136	73
	MU	89	19	442	75	285	200	98	195	81
	MV	105	38	1200	70	638	227	199	281	240
motor functions (except PI)	non-locomotor	55	16	1200	78	785	159	123	275	287
	locomotor	288	4	700	61	300	174	136	184	113
	swimming	53	18	442	50	282	183	131	169	98
	flying	25	4	363	19	165	79	87	100	78
	terrestrial	210	33	700	70	300	187	133	198	116

<sup>a</sup>Number of  $f$  values, minimum, maximum, quantile 10%, quantile 90%, median, interquartile range 25–75%, mean and standard deviation of  $f$ .

<sup>b</sup>This line M2 does not include myofibrils MF.

tension  $f$ , temperature, reference) are gathered in table 3 for molecular motors and table 4 for non-molecular motors. In table 3,  $f$  was calculated from the measured force or torque given in the references cited and the cross-sectional area and lever arm given in table 2. The statistics on  $f$  are summarized in table 5.

### 3.1. Specific tensions of molecular and non-molecular motors follow similar statistical distributions

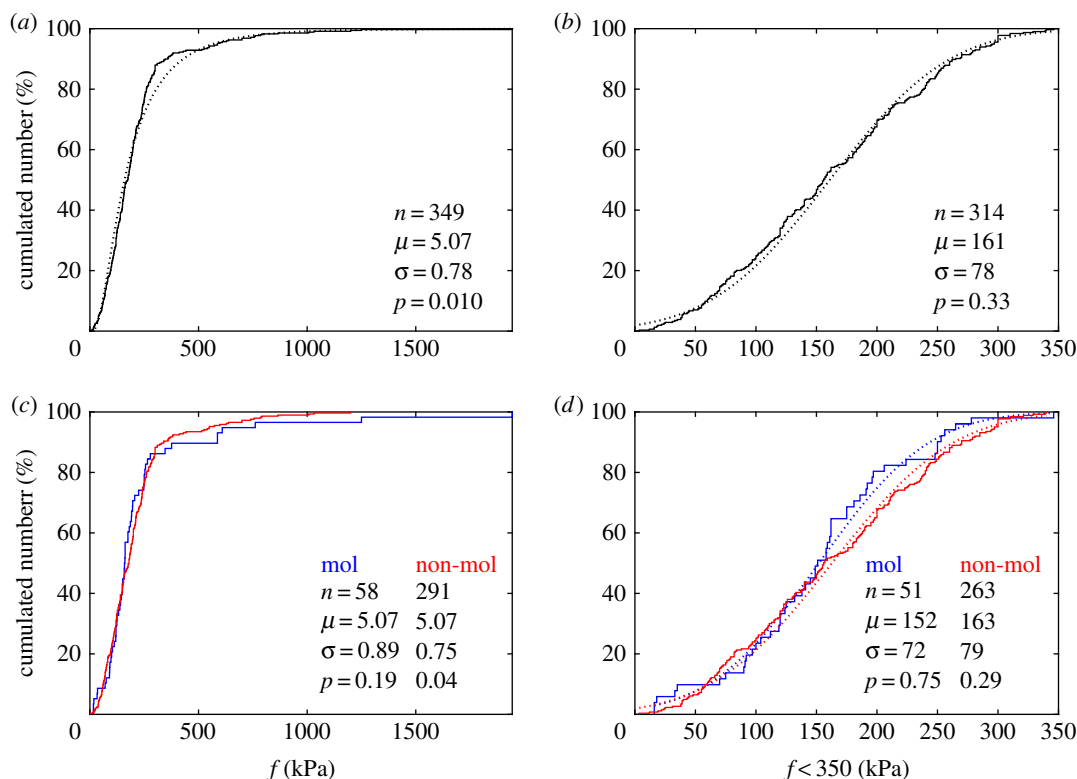
The distribution of all  $f$  values is close to lognormal, with  $\log_{10}(f)$  following approximately a normal distribution of mean  $\mu = 5.07$  (corresponding to 159 kPa), the largest measured tension (in a pilus) being 1900 kPa (figure 1a). Since the slope of the distribution changes rapidly for  $f = 350$  kPa, we have also plotted the distribution of  $f$  data smaller than this value (90% of the total), which follow very closely a normal distribution of mean  $\pm$  s.d. =  $161 \pm 78$  kPa (figure 1b). Figure 1c compares the tensions  $f$  of molecular and non-molecular motors, which follow distributions that are not significantly different, close to lognormal for all values and normal for  $f < 350$  kPa (figure 1d).

Motors developing tensions higher than 350 kPa are found in both microorganisms and large animals. In the former, the only ones are pili. In the latter, 23 of 29 (80%) are whole muscles measured *in vivo* (MV) in crustaceans (claw closers) and insects (jump muscles). We shall return to this point later.

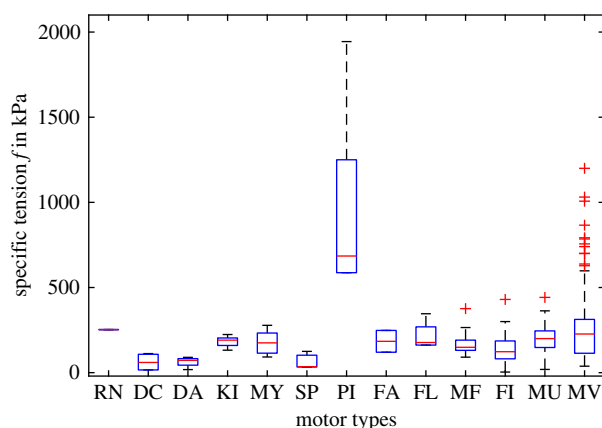
### 3.2. Differences exist depending on motor types, taxonomic groups and functional groups

Figure 2 shows that the tension for bacterial pili (PI, median 685 kPa, interquartile range (IQR) 663 kPa,  $n = 6$ ) is clearly an outlier with respect to all other motors (median 167 kPa, IQR 134 kPa,  $n = 343$ ). Therefore, in all the following comparisons, pili are excluded.

Comparisons of tension without pili per motor types, taxonomic groups and motor functions are shown as boxplots in figure 3 and the corresponding statistical tests (ANOVA and multiple comparison



**Figure 1.** Distributions of specific tensions  $f$ . (a) Empirical cumulated distribution function (CDF). All  $f$  values are shown along the  $x$ -axis as stepwise increments, giving a complete and undistorted view of the original data. Empirical CDF is fitted to a lognormal distribution of mean  $\mu$  and s.d.  $\sigma$  (dotted black line); fit is rejected at level 5% ( $p = 0.01$ ). (b) Empirical CDF of  $f < 350$  kPa (solid black line) with fitted normal distribution of  $\mu$  and  $\sigma$  in kPa (dotted black line), not rejected at level 5% ( $p = 0.33$ ). (c) Empirical CDFs of  $f$  for molecular motors (blue line, fitted lognormal not rejected) and non-molecular motors (red line, fitted lognormal rejected); the two distributions are not significantly different ( $p = 0.40$ ). (d) Empirical CDFs (solid line) and fitted normal CDFs (dotted line) for molecular (blue line) and non-molecular (red line) motors with  $f < 350$  kPa;  $\mu$  and  $\sigma$  in kPa; the two distributions are not significantly different ( $p = 0.20$ ). All comparisons based on Kolmogorov–Smirnov tests.



**Figure 2.** Boxplots of specific tensions per motor type ( $n = 349$ ). The boxes extend from the lower quartile to the upper quartile values with the medians (red line) in between. The whiskers extend to the most extreme data values within  $1.5 \times$  IQR. Outliers (red crosses) are tensions beyond the end of the upper whiskers. Motor types: RN, RNA polymerase ( $n = 1$ ); DC, cytoplasmic dynein (4); DA, axonemal dynein (4); KI, kinesin (7); MY, myosin (11); SP, spasmoneme (3); PI, pili (6); FA,  $F_0/F_1$  ATPase (2); FL, flagellum (4); MF, myofibril (16); FI, muscular fibre (97); MU, muscle *in vitro* (89); MV, muscle *in vivo* (105). ANOVA and multiple comparison of means (electronic supplementary material, table S1, motor types with  $n < 5$  removed: RN, DC, DA, SP, FA and FL): PI  $\neq$  (KI, MY, MF, FI, MU, MV), FI  $\neq$  MV and MU  $\neq$  MV. Pili PI are significantly different from all other motor types.



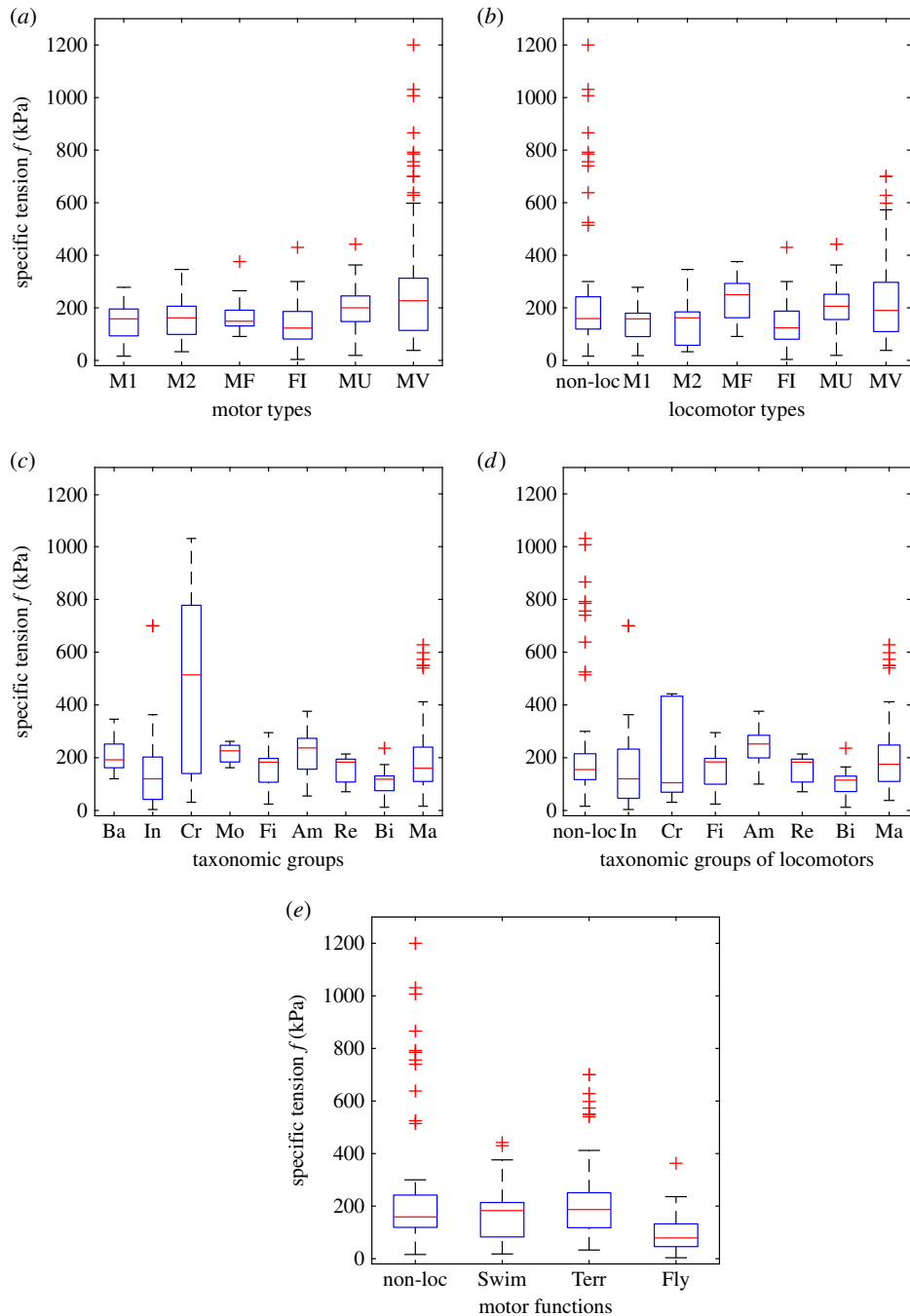


**Figure 3.** Boxplots of specific tensions of all motors except pili ( $n = 343$ ). Pili were excluded from molecular assemblies (M2), bacteria (Ba) and terrestrial motors (Terr). (a) Per motor type. Abbreviations and number of values per class as defined in figure 2, except M1, single molecule ( $n = 27$ ) and M2, molecular assembly ( $n = 9$ ). ANOVA and multiple comparison of means (electronic supplementary material, table S2):  $MV \neq (M1, FI, MU)$ . Among the 11 MV outliers, 9 are claw muscles and 2 are jump muscles. (b) Same as (a) with non-locomotors (non-loc,  $n = 55$ ) as a separate class. ANOVA and multiple comparison of means (electronic supplementary material, table S3):  $non-loc \neq (M1, FI)$  and  $FI \neq MV$ . (c) Taxonomic groups: Ba, bacteria ( $n = 7$ ); Pr, protozoa (4); Al, algae (1); Fu, fungi (1); Ec, echinoderms (1); Ar, arachnids (1); In, insects (19); Cr, crustaceans (19); Mo, molluscs (5); Fi, fish (29); Am, amphibian (31); Re, reptiles (5); Bi, birds (18); Ma, mammals (202). Groups with  $n < 5$  (protozoa, algae, fungi, echinoderms, arachnids) were removed (remaining data:  $n = 335$ ); ANOVA and multiple comparison of means (electronic supplementary material, table S4): crustaceans are significantly different from all other groups. (d) Same as (c) for locomotors ( $n = 275$ ) with non-locomotors ( $n = 48$ ) as a separate class. Groups with  $n < 5$  were removed (same as in (c), plus bacteria and molluscs). Insects ( $n = 17$ ), crustaceans (5), fishes (28), amphibians (25), reptiles (5), birds (17), mammals (178). ANOVA and multiple comparison of means (electronic supplementary material, table S5):  $non-loc \neq (Fi, Bi, Ma)$ . (e) Per motor function: non-locomotory ( $n = 55$ ), swimming (53), flying (25), terrestrial (210). Abbreviations and number of values per class as given in figure 1d, except for Terr ( $n = 210$ ). ANOVA and multiple comparison of means (electronic supplementary material, table S6):  $non-loc \neq (Swim, Terr, Fly)$  and  $Fly \neq Terr$ .

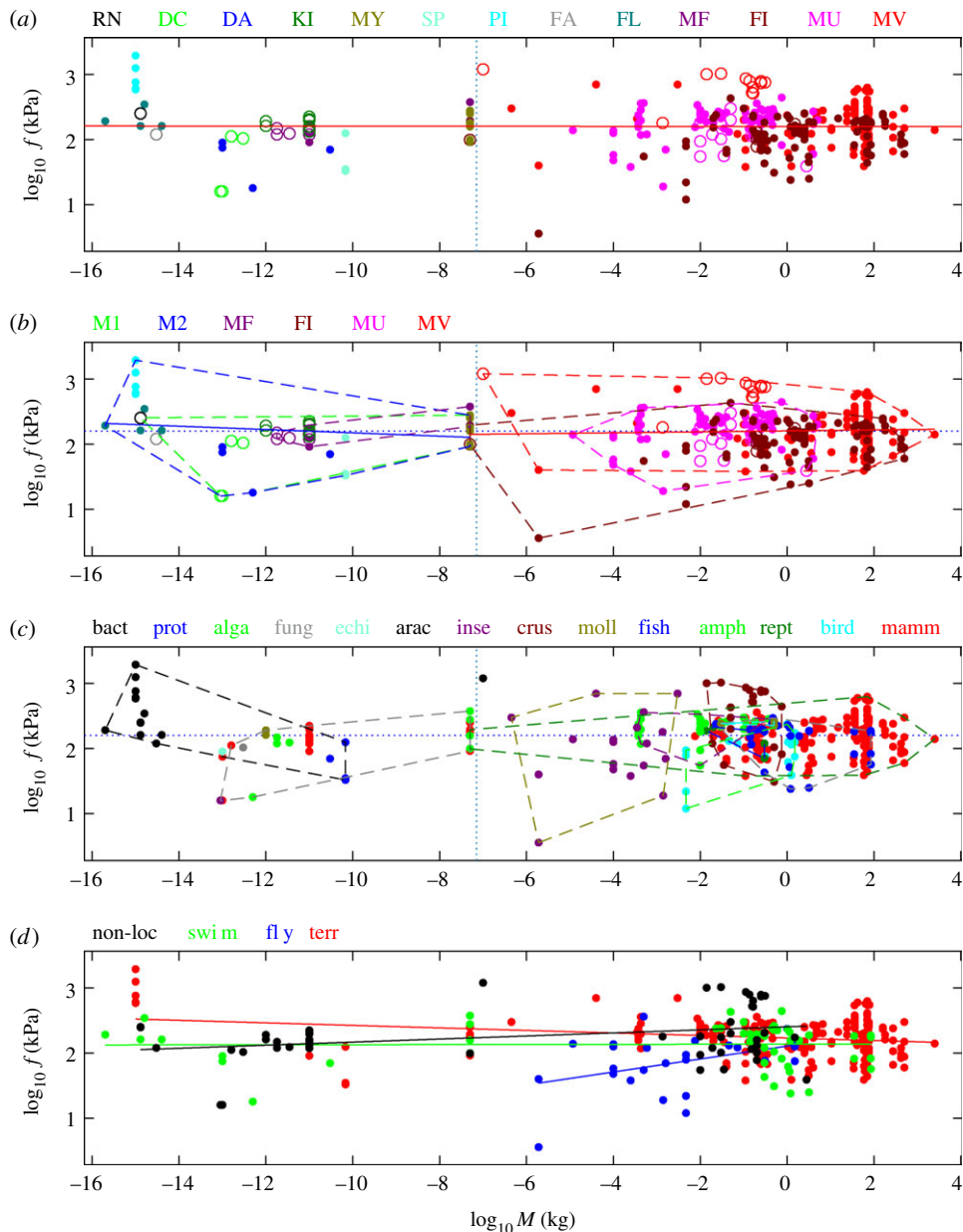


**Figure 4.** Log–log plot of specific tension versus cell or body mass. (a) Locomotors shown as points ( $n = 294$ ) and non-locomotors as circles ( $n = 55$ ). Regression line of all  $\log_{10} f$  versus  $\log_{10} M$  (solid red line, slope  $-5 \times 10^{-4}$  not significantly different from zero,  $p = 0.90$ ). Regression line of locomotors (slope  $-6 \times 10^{-3}$  not significantly different from zero,  $p = 0.24$ ) indistinguishable from red line, not shown (see the electronic supplementary material, table S7). Vertical dotted line: mass of cells on the left, of multicellular organisms on the right. Motor types: abbreviations and number of values per type as defined in figure 2. (b) Motor types: same abbreviations and numbers as in (a), except M1, single molecule ( $n = 27$ ) and M2, molecular assembly (15 with pili). Symbols and colours of points as in (a). Points belonging to the same motor type located within the convex polygons shown. Regression lines of molecular motors (M1, M2 and MF, blue line on the left, slope  $-0.03$  not significantly different from zero,  $p = 0.17$ ) and non-molecular motors (FI, MU, MV, red line on the right, slope  $7 \times 10^{-3}$  not significantly different from zero,  $p = 0.47$ ). For these and other regressions on motor types, see the electronic supplementary material, tables S7–S9. Horizontal dotted blue line is mean  $\log_{10} f$  (kPa) = 2.2. Vertical dotted blue line as in (a). (c) Taxonomic groups: abbreviations and number of values per class as given in figure 3c, except for bacteria ( $n = 13$  with pili). On the left side, polygons enclose motors from single cells (black) and from multicellular organisms (grey). For regressions on taxonomic groups, see the electronic supplementary material, tables S10 and S11. Horizontal and vertical dotted lines as in (b). (d) Motor functions: non-locomotory ( $n = 55$ ), swimming (53), flying (25), terrestrial (216 with pili). Their respective regression lines are shown; their slopes  $s$  are significantly different from zero (non-loc,  $s = 0.02$ ,  $p = 0.02$ ; Fly,  $s = 0.1$ ,  $p = 0.05$ ; Terr,  $s = -0.02$ ,  $p < 10^{-3}$ ) except Swim ( $s = 8 \times 10^{-4}$ ,  $p = 0.93$ ), see the electronic supplementary material, table S12. In all panels, the scale on the y-axis is 1.5 times larger than on the x-axis.

of means) are given in the electronic supplementary material, tables S1–S6. Figure 3*a,b* for motor types indicates that muscles *in vivo* significantly differ from single molecules M1, fibres and muscles *in vitro*, essentially because of the large tensions of non-locomotor muscles. Comparisons of taxonomic groups with number of  $f$  values greater than or equal to 5 (pili excluded) show that crustaceans differ from all other groups (all motors, figure 3*c*). Finally, comparison of motor functions show that motors used for flight have specific tensions significantly different from those of motors used for moving the organisms on (or with respect to) a solid substrate and non-locomotors differ from all three kinds of locomotors (figure 3*e*).

### 3.3. There is no large-scale variation with cell or body mass

Log–log plots of the 329 pairs of  $(M, f)$  values are shown in figure 4. Overall, values of cell and body mass  $M$  range from  $2 \times 10^{-16}$  kg (bacterium) to 2500 kg (elephant), whereas values of specific tension  $f$  range from 3.6 to 1944 kPa. Hence, whereas  $M$  varies by more than 19 orders of magnitude,  $f$  only varies by a factor of 500. For easier reading, polygons enclosing all points of the same category are shown: types of motors (figure 4*b*) and taxonomic groups (figure 4*c*).

Overall, there is no large-scale variation with cell or body mass. Indeed, the power law regression calculated for the entire dataset is  $f = 159 M^\alpha$  with  $\alpha = -0.5 \times 10^{-3} \pm 7.7 \times 10^{-3}$  (95% confidence limits  $-8.2 \times 10^{-3}$ ,  $7.2 \times 10^{-3}$ ), this slope is not significantly different from zero ( $p = 0.90$ , figure 4*a*). The slope is not either different from zero for data restricted to molecular motors (M1, M2 and MF,  $f = 83 M^\alpha$  with  $\alpha = -0.025 \pm 0.037$ ,  $p = 0.17$ , figure 4*b* on the left) and non-molecular motors (FI, MU, MV,  $f = 159 M^\alpha$  with  $\alpha = 0.0073 \pm 0.020$ ,  $p = 0.47$ , figure 4*b* on the right). Complete description and test of these global regressions are given in the electronic supplementary material, table S7.

We also looked for ‘local’ trends based on the different categories defined previously. For motor types, some slight positive and negative slopes of the regression lines  $f$  versus  $M$  were found (electronic supplementary material, tables S8 and S9). For taxonomic groups (electronic supplementary material, tables S10 and S11) and motor functions (electronic supplementary material, table S12), either the slope is not significantly different from zero (according to the  $F$ -test at level 1%), or the slope is smaller or equal to 0.02 in absolute value.

## 4. Discussion

We discuss in order the choice of specific tension for normalizing forces developed by widely different motors, the similarity of specific tension in molecular and non-molecular motors, the factors explaining the variability of tension, especially in muscles, and the relationship between tension invariance and force–mass scaling.

### 4.1. Specific tension as a size-independent measure of force

In order to compare forces developed by biological motors as different as molecules and muscles, whose spatial scale varies by nearly 7 orders of magnitude and whose applied force varies by nearly 14 orders of magnitude, it is useful to express them in relative values. Because most non-molecular motor forces  $F$  (FI, MU, MV) are expressed as specific tension ( $F/A$ ) in the literature, it is natural to try to express molecular motors similarly.

As  $F/A$  is not available for molecular motors, in order to avoid bias, we defined the cross-section  $A$  in the most basic way, i.e. from the volume  $V$  as  $A = V^{2/3}$ , which holds for a cube and still holds in order of magnitude for shapes of moderate elongation. This is in line with results of Marden & Allen [18] who found  $F$  proportional to motor mass  $m^{2/3}$  for a class of molecular motors, and to the fact that these forces depend on chemical bonds (mainly hydrogen bonds), whose number acting in parallel is expected to depend on the cross section. For defining the cross-section, we were extremely careful to select the acting part of the motor (ignoring the ‘passive’ tails) so that the shape was of moderate elongation. For example to estimate the volume of the myosin motor, we only considered the heads and ignored the tail which does not contribute to the actin–myosin interaction. We will return to this topic in the last subsection ‘Scaling with motor’s mass’ and suggest below an order-of-magnitude interpretation.

## 4.2. Invariance of specific tension in molecular and non-molecular motors

The main characteristics found here for the values of tension  $f$  in both molecular (M1, M2, MF) and non-molecular motors (FI, MU, MV) are (table 5): (i) their almost equal median tensions (approx. 170 kPa), (ii) their similar ranges of variation ( $60 < f < 350$  kPa for 90% of motors), and (iii) the approximately five times higher tensions exerted by pili ( $600 < f < 2000$  kPa). These three characteristics can be understood from basic physical considerations.

### 4.2.1. Molecular motors

Molecular motors are proteins that produce mechanical energy by changing their three-dimensional conformation. They move in steps whose length is of the order of magnitude of their size  $a_0$ , which is typically  $a_0 \sim 6$  nm [195,196]. The steps are mainly powered by ATP with free energy  $W_0 \simeq 12kT \simeq 0.5 \times 10^{-19}$  J/molecule at  $T = 300$  K [197]. Therefore, the elementary force  $F_0$  developed by motor proteins is of order of magnitude  $F_0 \sim W_0/a_0 \sim 8$  pN and the corresponding force per unit cross-sectional area  $f$  is  $f \sim F_0/a_0^2 \simeq W_0/a_0^3 \sim 200$  kPa. This is close to the average value found for molecular motors (M1, M2 and MF, table 5). This order-of-magnitude estimate is based on a perfect transduction of chemical into mechanical energy. Taking into account the actual efficiency would not change this order of magnitude since molecular motors are known to have a high efficiency—often exceeding 50% (e.g. [198,199]), in particular, 80–95% for kinesin [197] and up to 100% for F1-ATPase [8].

Molecular motors, like other proteins, owe their properties to a three-dimensional structure mainly held by H-bonds and other weak forces [200,201]. In order to act near (but not at) thermal equilibrium and not to break the motor protein, the elementary motor force should not exceed  $kT$  divided by the distance over which H-bonds operate, i.e. the size of the water molecule,  $a_{\text{H}_2\text{O}} \simeq 0.3$  nm. This yields the minimum size,  $a_0 > a_{\text{H}_2\text{O}} \times (W_0/kT) \simeq 4$  nm, and maximum tension,  $f \simeq W_0/a_0^3 < 800$  kPa, of molecular motors. This order of magnitude estimate is similar to the maximum tension observed in molecular motors (table 5) with the notable exception of pili.

Pili, which are virtually universal in prokaryotes [202], have exceptional mechanical properties of stretching and adhesion, and some of them can withstand extreme forces, with an important role played by covalent bonds (e.g. [203]) so that the above order-of-magnitude estimate, based on weak forces, does not apply to them. In order to compare pili with other structures, we have only considered steady-state unwinding forces (e.g. [60]). Even then, pili can still reach extreme specific tensions, with a median four times higher than that of other motors.

### 4.2.2. Non-molecular motors

The most striking result of this paper is that the formally defined tension of molecular motors turns out to be similar to the value  $f \simeq 200$  kPa typical of muscle fibres. A hint to this uniformity stems from the basic arrangement of myosin motors in striated muscles (reviewed in e.g. [13,204]). Most of the space within muscle fibres is occupied by protein thick filaments along which groups of myosin globular motors (heads) are protruding with an axial spacing  $e = 14.6$  nm. These motors are cyclically attaching to (and detaching from) adjacent thin filaments of actin to form the cross-bridges, and enable thin and thick filaments to slide past each other. Along each half thick filament (of total length  $2l \simeq 1.6$   $\mu\text{m}$ , neglecting for this order-of-magnitude estimate a bare zone of smaller length free of motors) about 150 myosin molecules exert forces that add in parallel and only about one-third of the cross-bridges are attached during isometric contraction [47,205]. Therefore, the number of active individual myosin motors along each half thick filament is  $N \simeq 50$ . (Note that since  $l/e \simeq 50$ , this might imply that only one motor per group of three can attach simultaneously, a likely consequence of steric constraints brought about by the three-dimensional structure enabling transitory conformational changes.) With  $N$  motors acting in parallel each exerting a force  $F_{\text{myosin}}$  the total force per thick filament is  $NF_{\text{myosin}}$ . Each thick filament and its associated lattice of thin filaments occupies an equivalent cross-section  $s \simeq d^2$ , where  $d \simeq 40$  nm is the lateral spacing of thick filaments, so the total tension in the structure is  $f_{\text{fibre}} \simeq NF_{\text{myosin}}/s$  which acts (in series) along the length of the fibre. Tables 3 and 4 show that the myosin motor, of equivalent cross-sectional area  $A \simeq 36$  nm<sup>2</sup>, exerts a mean force  $F_{\text{myosin}} \simeq f_{\text{myosin}}A \simeq 7$  pN. Substituting the values of  $F_{\text{myosin}}$ ,  $N$  and  $s$  in the above formula yields the tension in the structure  $f_{\text{fibre}} \simeq 240$  kPa.

This rough estimate enables us to understand why the tension of muscles ( $\simeq f_{\text{fibre}}$ ) is of the same order of magnitude as the tension of the myosin motor  $f_{\text{myosin}} \simeq 190$  kPa. Indeed, the tensions of muscle fibres and of myosin motors are in the ratio  $f_{\text{fibre}}/f_{\text{myosin}} \simeq NA/s$ , and the myosin motors are arranged so that the number  $N$  of them acting simultaneously in parallel is approximately equal to the ratio  $s/A$  of

the equivalent cross-sectional area of each thick–thin filament structure to that of an individual myosin motor head, which is not surprising because of steric constraints.

### 4.3. Origins of variability of specific tension in various motors

Overall, tensions in most molecular and non-molecular motors are distributed around their means according to similar Gaussian functions with coefficients of variation s.d./mean  $\simeq 0.5$ . This variability may arise from methodological, experimental and biological factors.

#### 4.3.1. Methodological and experimental factors

The cross-section  $A$  of molecular motors was estimated from their mass  $m$  using the formulae  $A = V^{2/3}$  and  $V = m/\rho$  with protein density  $\rho \simeq 10^{-3} \text{ pg nm}^{-3}$ . This is admittedly rough, since the longer dimension of the motors considered can differ from the cross-diameter by nearly a factor of 2. The resulting error may not be negligible compared with the observed variability of specific tension in molecular motors, in which more than 80% of  $f$  values are within one-third of the median and twice the median (see Q10, Q90 and median in table 5, second line).

Although we did not have to estimate the cross-section for muscles, their tensions show the same variability on  $f$  as molecular motors (Q10 is one-third the median and Q90 twice the median, see table 5, third line). Their cross-sectional area has sometimes been corrected for the area occupied by mitochondria (dragonfly, [116]), sometimes not (beetle, [115]) and never for the sarcoplasmic reticulum (e.g. [206]). The pennation angle has not always been taken into account. Temperature during the experiments has been noted and is usually close to the working temperature of the muscle. Although data are not fully homogeneous, the similarity of the distributions of specific tensions measured *in vivo* and *in vitro* suggests that uncorrected factors do not introduce important bias. In principle, corrections for these factors should lead to less variable data. However, no corrections have been attempted for two reasons. First, the information needed is not always provided, so corrections cannot be done systematically. Second, these corrections would probably have no incidence on the qualitative conclusions, and might even be less convincing than unmodified data.

Isometric tension in single skeletal muscle fibres (FI) is approximately 35% smaller than in whole muscles (MU or MV) (figure 3*a*). This difference probably results from the experimental conditions, most measurements of single fibres being performed after chemical or mechanical skinning. It produces swelling of the fibres and reduces the specific tension. Median tension is about the same for whole muscles when measured *in vitro* (MU, 200 kPa) and *in vivo* (MV, 227 kPa) (figure 3*a,b*). This indicates that the tension for muscles in behaving animals is close to the maximum they can develop in *in vitro* conditions.

It must also be realized that detailed physiologically and ecologically relevant comparisons between similar motors in different taxonomic groups are hindered by their unequal levels of investigation; for example, muscles MU have been studied in 29 vertebrate species, but only 13 invertebrate species (table 4).

#### 4.3.2. Biological factors

Further sources of variability are probably biological. At the molecular level, variability stems from differences within and across families of single motor proteins (M1). At the supramolecular level, notably in propulsion organelles and muscles, elementary molecular forces are expressed via an organization that introduces further variations and specific adaptations to the diversity of mechanical problems they had to solve. More factors being involved, the values of their tension is *a priori* less easy to predict, explaining the variability observed. Nonetheless, as shown in figure 3*a*, after removal of pili, the variability of specific tension between the different types of molecular motors studied is larger in motors M1 and M2 than in myofibrils. The structural and functional homogeneity of myofibrils contrasts with the heterogeneity of the other molecular motors.

Neglecting experimental errors and pili being set aside, tensions of non-molecular motors (FI, MU, MV) vary approximately in the same range as tensions of molecular motors (M1, M2 and MF) with the same statistical distribution (figure 1*c,d*). So, notwithstanding their myosin-based molecular homogeneity, the diversity in geometry and adaptation of muscular motors leads to variations in tension equivalent to those resulting from the diversity of molecules and their arrangements in molecular motors. It is remarkable that so many different mechanisms lead to the same final distributions of force per cross-sectional area at the microscopic and macroscopic levels.

#### 4.4. Variability of tensions in whole muscles

The variability of tension in muscles has been the subject of thorough research. An important adaptive factor is sarcomere length. As predicted by the sliding filament model of muscle contraction, long filaments and long overlap between thick and thin filaments should occur in fibres with long sarcomeres. As in long overlap zones more actin–myosin cross-bridges should be formed, the maximum tension which a fibre can produce should be correlated with sarcomere length [207,208]. The resting sarcomere length exhibits little variation in insect and vertebrate muscles (2–4  $\mu\text{m}$ ), but much greater variations in crustacean muscles (7–17  $\mu\text{m}$ ). Overall, tension scales isometrically with the resting sarcomere length [157]. In particular, the claw closer muscles of cancer crabs exhibit both the longest sarcomere lengths and extreme mean crushing forces (525–1030 kPa; table 4 and figure 3c). This is a special adaptation of shell-crushing non-locomotory motors which is not found in locomotors (figure 3d).

Many other factors have been invoked to explain the variations in muscle tension, such as the density of the myosin filaments, the non-uniformity of sarcomere length along the fibres, the diameter of myofibrillar bundles, the actin : myosin filament ratios and the cross-bridge duty factors. For example, the slightly higher tension than in other groups found in amphibians and molluscs (except crustaceans; figure 3c) may be explained by their higher proportion of fast oxidative fibres and their higher relative myofibrillar volume [4,206]. However, these various factors apparently play a minor role in arthropod and vertebrate muscles as more than 80% of the variation in muscle tension in a series of muscles from these groups can be explained by the resting sarcomere length ([157] and references therein).

Two characteristics other than tension contribute to muscle performance: speed of contraction (and relaxation) and endurance. They influence tension because high tension requires that most of the cross-sectional area of a fibre be myofibrils, whereas high endurance requires a large mitochondrial volume and short twitch duration requires an extended sarcoplasmic reticulum. Therefore, trade-offs are inherent in the functional design of muscles so that a muscle cannot be simultaneously strong, enduring and rapid. This is the reason why rapid muscles are weak (either enduring, e.g. katydid singing muscles, or not, e.g. lobster sound-producing muscles with their hypertrophied SR) [208]. However, special adaptations in the oscillatory (asynchronous) flight muscles of insects result in high contraction frequencies without a large volume of SR, which leaves room for more mitochondria, but their strength is nevertheless limited by the endurance requirements of flight [208]. They are built optimally for maximum output of energy in their narrow contraction range, whereas most vertebrate sarcomeres are optimized for optimal mechanical conversion of chemical energy across a wider contraction range [209]. These different adaptations contribute to the variability observed. Overall, the similarity of muscle tensions is essentially owing to the similarity of fibre structure and thick filament length across muscles and species, in contrast with the variability of muscle speeds which are affected by the variability of thin filament lengths (e.g. [210]).

It is remarkable that tension is smaller in flight locomotors (median 79 kPa) than in terrestrial locomotors (median 187 kPa) and in swim locomotors (183 kPa), although only the difference for terrestrial locomotors is significant according to ANOVA at level 5% (figure 3e). Despite the high power needed for flight, the high frequencies required may impose a large concentration of mitochondria and, at least in birds, of sarcoplasmic reticulum at the expense of myofibrils. Solving this issue will need further investigation.

#### 4.5. Absence of large-scale trend with cell's or body's mass

Given the constancy in both central value (mean or median) and dispersion (s.d. or interquartile range) of  $f$  in molecular and non-molecular motors, it is not surprising that the regressions in a log–log plot of  $f$  against  $M$ , the mass of the cell (for subcellular motors) or body (for cellular and supracellular motors) from which the motor is extracted, give no evidence of overall trend (figure 4a,b). Other variables for the mass might be used, but their implementation is difficult because they are often ill-defined or unknown. This is the reason why we chose for the horizontal axis a proxy of the mass that the motor moves—the mass of the next higher hierarchical level, i.e. the cell's mass for subcellular motors (M1, M2, MF) and the animal's mass for cellular and supracellular motors (FI, MU, MS). This definition is simple, unambiguous, known in almost all cases and discriminant with a range extending over 18 orders of magnitude. If we had chosen the motor's mass  $m$  for the horizontal axis, the range would have been still wider since the minimum mass would be  $10^{-22}$  kg (kinesin) and the maximum mass  $> 1$  kg (muscle), so that as the overall range of  $f$  would remain the same, the slope of the regression line would become still closer to zero.

The absence of global trends does not preclude the existence of ‘local’ trends, i.e. regression lines with slope significantly different from zero, for specific classes of motors extending on a narrower mass range. Several examples of such significant trends were found (see the electronic supplementary material, tables S8–S12) but their slopes are small and difficult to interpret. These small-scale relationships are outside the scope of this paper which focuses on a large-scale study. The wide range of size, mass and area considered allows one to transcend the possible variations specific to certain categories.

#### 4.6. Scaling with motor’s mass

A different approach based on force  $F$  and motor mass  $m$  strengthens this conclusion. Indeed, Marden & Allen [18] studied the scaling of forces with motor’s mass for two classes of animal- and human-made motors and found that one of them, ‘Group 1’ motors, producing translational motion, scale allometrically with motor mass  $m$ , as  $F \simeq 10^3 m^{2/3}$  (with  $F$  in Newtons and  $m$  in kilograms). We show below that this scaling, expressed in terms of specific tension  $f$ , is in good agreement with the typical specific tension found in the present paper (approx. 200 kPa). Consider first the order-of-magnitude approximation of cubes of section  $A$ . With the mass density  $\rho \simeq 10^3 \text{ kg m}^{-3}$ , the motor mass is  $m \simeq \rho A^{3/2}$ , so that the scaling above  $F \simeq 10^3 (\rho A^{3/2})^{2/3}$  yields the tension  $f = F/A \simeq 10^3 \rho^{2/3} \simeq 100 \text{ kPa}$ . This is a minimum value since replacing the cubic approximation by an elongated shape, with a ratio length/width  $r$ , with width  $d \simeq A^{1/2}$ , would yield  $m \simeq r \rho A^{3/2}$ , whence  $f \simeq 100 r^{2/3} \text{ kPa}$ . Thus, the mass–force scaling for Group 1 motors found by Marden & Allen [18] implies the constancy of their specific tension with a constant value consistent with that found here.

The above argument might also explain why three ‘molecular motors’ corresponding in part to our ‘M2 motors’ (bacterial flagellum, mammalian flagellum and spasmoneme) are shifted to the right of the fitted line (see red circles in fig. 1 of [18]). Indeed, the mass  $m$  considered is the mass of the whole organelle, whose length far exceeds the square root of the section (i.e.  $r \gg 1$ ). This implies that  $m$  is much larger than  $\rho A^{3/2}$ , so that a constant value of  $f$  yields a smaller value of  $F/m^{2/3}$ .

However, for the other group of motors (Group 2) defined by Marden & Allen [18], the biological motor forces are generally deduced from the motion of the whole organism against gravity, which implies various joints and lever arms connecting the motor to the organism. It is, therefore, difficult to compare these data with those considered in this paper, which are directly measured at the level of the muscle (or of the fibre or the molecular motor).

### 5. Concluding remarks

The main result of this paper is that, despite their diversity, molecular and macroscopic biological motors do exert similar forces per unit cross-sectional area, which enables us to unify biological motors of different sizes and varied functions, from the motion of animals and microorganisms to cargo transport in cells or DNA transcription. The similarity of tensions of macroscopic muscles and fibres is not surprising as it stems from the similarity of fibres’ basic architecture. In turn, the similarity of the tensions of molecular motors is owing to the basic physical properties of protein machines, and we have given an order-of-magnitude estimate of this tension from basic physics. Finally, we have shown that the tension in muscle fibres is similar to that of the myosin motor in particular because of the arrangement of these motors in the fibres, owing to steric constraints.

The approximate constancy of the maximum force per unit area  $f$  found in this paper from molecules to muscles implies general scaling laws for the motion of organisms [211] and raises the question of relating these laws to basic biological and physical constraints. Moreover, it calls for an explanation of why human-engineered motors, which are not based on ATP hydrolysis and hydrogen bond forces, show very similar specific tension to biological motors [18,19].

**Data accessibility.** All supporting data are made available in tables 2–5 and the electronic supplementary material, tables S1–S12.

**Authors’ contributions.** J.-P.R. and N.M.-V. each made significant and substantial contributions to this study in terms of the conception, design, data collection and interpretation of results, as well as preparing the manuscript. J.-P.R. made the statistical analyses.

**Competing interests.** We declare we have no competing interests.

**Funding.** We received no funding for this study.

## References

- Close R. 1972 Dynamic properties of mammalian skeletal muscles. *Physiol. Rev.* **52**, 129–197.
- Alexander RM. 1985 The maximum forces exerted by animals. *J. Exp. Biol.* **115**, 231–238.
- Ruegg JC. 1968 Contractile mechanisms of smooth muscle. *Symp. Soc. Exp. Biol.* **22**, 45–66.
- Medler S. 2002 Comparative trends in shortening velocity and force production in skeletal muscles. *Am. J. Physiol. Regul. Integr. Comp. Physiol.* **283**, R368–R378. (doi:10.1152/ajpregu.00689.2001)
- Tesi C, Colombo F, Nencini S, Piroddi N, Poggesi C. 2000 The effect of inorganic phosphate on force generation in single myofibrils from rabbit skeletal muscle. *Biophys. J.* **78**, 3081–3092. (doi:10.1016/S0006-3495(00)76845-7)
- Mehta AD, Rief M, Spudich JA, Smith DA, Simmons RM. 1999 Single-molecule biomechanics with optical methods. *Science* **283**, 1689–1695. (doi:10.1126/science.283.5408.1689)
- Sambongi Y, Iko Y, Tanabe M, Omote H, Iwamoto-Kihara A, Ueda I, Yanagida T, Wada Y, Futai M. 1999 Mechanical rotation of the c subunit oligomer in ATP synthase ( $F_0F_1$ ): direct observation. *Science* **286**, 1722–1724. (doi:10.1126/science.286.5445.1722)
- Yasuda R, Noji H, Kinoshita, Jr K, Yoshida M. 1998 F1-ATPase is a highly efficient molecular motor that rotates with discrete 120° steps. *Cell* **93**, 1117–1124. (doi:10.1016/S0092-8674(00)81456-7)
- Berg HC. 2003 The rotary motor of bacterial flagella. *Annu. Rev. Biochem.* **72**, 19–54. (doi:10.1146/annurev.biochem.72.121801.161737)
- Biais N, Ladoux B, Higashi D, So M, Sheetz M. 2008 Cooperative retraction of bundled type IV pili enables nanonewton force generation. *PLoS Biol.* **6**, e87. (doi:10.1371/journal.pbio.0060087)
- Miller E, Garcia T, Hultgren S, Oberhauser AF. 2006 The mechanical properties of *E. coli* type I pili measured by atomic force microscopy techniques. *Biophys. J.* **91**, 3848–3856. (doi:10.1529/biophysj.106.088989)
- Upadhyaya A, Baraban M, Wong J, Matsudaira P, van Oudenaarden A, Mahadevan L. 2008 Power-limited contraction dynamics of *Vorticella convallaria*: an ultrafast biological spring. *Biophys. J.* **93**, 265–272. (doi:10.1529/biophysj.107.108852)
- Craig R, Woodhead JL. 2006 Structure and function of myosin filaments. *Curr. Opin. Struct. Biol.* **16**, 204–212. (doi:10.1016/j.sbi.2006.03.006)
- Schmitz KA, Holcomb-Wygle DL, Oberski DJ, Lindemann CB. 2000 Measurement of the force produced by an intact bull sperm flagellum in isometric arrest and estimation of the dynein stall force. *Biophys. J.* **79**, 468–478. (doi:10.1016/S0006-3495(00)76308-9)
- Schnitzer MJ, Visscher K, Block SM. 2000 Force production by single kinesin motors. *Nat. Cell Biol.* **2**, 718–723. (doi:10.1038/35036345)
- Gennerich A, Carter AP, Reck-Peterson SL, Vale RD. 2007 Force-induced bidirectional stepping of cytoplasmic dynein. *Cell* **131**, 952–965. (doi:10.1016/j.cell.2007.10.016)
- Wang MD, Schnitzer MJ, Yin H, Landick R, Gelles J, Block SM. 1998 Force and velocity measured for single molecules of RNA polymerase. *Science* **282**, 902–907. (doi:10.1126/science.282.5390.902)
- Marden JH, Allen LR. 2002 Molecules, muscles, and machines: universal performance characteristics of motors. *Proc. Natl Acad. Sci. USA* **99**, 4161–4166. (doi:10.1073/pnas.022052899)
- Marden JH. 2005 Scaling of maximum net force output by motors used for locomotion. *J. Exp. Biol.* **208**, 1653–1664. (doi:10.1242/jeb.01483)
- Mooney RA, Landick R. 1999 RNA polymerase unveiled. *Cell* **98**, 687–690. (doi:10.1016/S0092-8674(00)81483-X)
- Reck-Peterson SL, Yildiz A, Carter AP, Gennerich A, Zhang N, Vale RD. 2006 Single-molecule analysis of dynein processivity and stepping behavior. *Cell* **126**, 335–348. (doi:10.1016/j.cell.2006.05.046)
- Carter AP, Cho C, Jin L, Vale RD. 2011 Crystal structure of the dynein motor domain. *Science* **331**, 1159–1165. (doi:10.1126/science.1202393)
- Block SM. 1998 Kinesin: what gives? *Cell* **93**, 5–8. (doi:10.1016/S0092-8674(00)81138-1)
- Rayment I, Holden HM, Whittaker M, Yohn CB, Lorenz M, Holmes KC, Milligan RA. 1993 Structure of the actin-myosin complex and its implications for muscle contraction. *Science* **261**, 58–65. (doi:10.1126/science.8316858)
- Rayment I, Holden HM. 1994 The three-dimensional structure of a molecular motor. *Trends Biochem. Sci.* **19**, 129–134. (doi:10.1016/0968-0004(94)90206-2)
- Goldman YE. 1998 Wag the tail: structural dynamics of actomyosin. *Cell* **93**, 1–4. (doi:10.1016/S0092-8674(00)81137-X)
- Billington N, Revill DJ, Burgess SA, Chantler PD, Knight PJ. 2014 Flexibility within the heads of muscle myosin-2 molecules. *J. Mol. Biol.* **426**, 894–907. (doi:10.1016/j.jmb.2013.11.028)
- Yoshida M, Muneyuki E, Hisabori T. 2001 ATP synthase: a marvelous rotary engine of the cell. *Nat. Rev.* **2**, 669–677. (doi:10.1038/35089509)
- Hoffmann J *et al.* 2010 ATP synthases: cellular nanomotors characterized by LILBID mass spectrometry. *Phys. Chem. Chem. Phys.* **12**, 13 375–13 382. (doi:10.1039/c0cp00733a)
- Reid SW, Leake MC, Chandler JH, Lo C-J, Armitage JP, Berry RM. 2006 The maximum number of torque-generating units in the flagellar motor of *Escherichia coli* is at least 11. *Proc. Natl Acad. Sci. USA* **103**, 8066–8071. (doi:10.1073/pnas.0509932103)
- Minamino T, Imada K, Namba K. 2008 Molecular motors of the bacterial flagella. *Curr. Opin. Struct. Biol.* **18**, 693–701. (doi:10.1016/j.sbi.2008.09.006)
- Gross SP, Welte MA, Block SM, Wieschaus EF. 2000 Dynein-mediated cargo transport *in vivo*: a switch controls travel distance. *J. Cell Biol.* **148**, 945–955. (doi:10.1083/jcb.148.5.945)
- Toba S, Watanabe TM, Yamaguchi-Okimoto L, Toyoshima YY, Higuchi H. 2006 Overlapping hand-over-hand mechanism of single molecular motility of cytoplasmic dynein. *Proc. Natl Acad. Sci. USA* **103**, 5741–5745. (doi:10.1073/pnas.0508511103)
- Mallik R, Carter BC, Lex SA, King SJ, Gross SP. 2004 Cytoplasmic dynein functions as a gear in response to load. *Nature* **427**, 649–652. (doi:10.1038/nature02293)
- Hirakawa E, Higuchi H, Toyoshima YY. 2000 Processive movement of single 22S dynein molecules occurs only at low ATP concentrations. *Proc. Natl Acad. Sci. USA* **97**, 2533–2537. (doi:10.1073/pnas.050585297)
- Sakakibara H, Kojima H, Sakai Y, Katayama E, Oiwa K. 1999 Inner-arm dynein c of *Chlamydomonas* flagella is a single-headed processive motor. *Nature* **400**, 586–590. (doi:10.1038/23066)
- Shingyoji C, Higuchi H, Yoshimura M, Katayama E, Yanagida T. 1998 Dynein arms are oscillating force generators. *Nature (Lond.)* **393**, 711–714. (doi:10.1038/31520)
- Holcomb-Wygle DL, Schmitz KA, Lindemann CB. 1999 Flagellar arrest behavior predicted by the geometric clutch model is confirmed experimentally by micromanipulation experiments on reactivated bull sperm. *Cell Motil. Cytoskeleton* **44**, 177–189. (doi:10.1002/(SICI)1097-0169(199911)44:3<177::AID-CM3>3.0.CO;2-W)
- Svoboda K, Block SM. 1994 Force and velocity measured for single kinesin molecules. *Cell* **77**, 773–784. (doi:10.1016/0092-8674(94)90060-4)
- Visscher K, Schnitzer MJ, Block SM. 1999 Single kinesin molecules studied with a molecular force clamp. *Nature* **400**, 184–189. (doi:10.1038/22146)
- Higushi H, Muto E, Inoue Y, Yanagida T. 1997 Kinetics of force generation by single kinesin molecules activated by laser photolysis of caged ATP. *Proc. Natl Acad. Sci. USA* **94**, 4395–4400. (doi:10.1073/pnas.94.9.4395)
- Hunt AJ, Gittes F, Howard J. 1994 The force exerted by a single kinesin molecule against a viscous load. *Biophys. J.* **67**, 766–781. (doi:10.1016/S0006-3495(94)80537-5)
- Meyhöfer E, Howard J. 1995 The force exerted by a single kinesin molecule against an elastic load. *Proc. Natl Acad. Sci. USA* **92**, 574–578. (doi:10.1073/pnas.92.2.574)
- Kojima H, Muto E, Higuchi H, Yanagida T. 1997 Mechanics of single kinesin molecules measured by optical trapping nanometry. *Biophys. J.* **73**, 2012–2022. (doi:10.1016/S0006-3495(97)78231-6)
- Jamison DK, Driver JW, Rogers AR, Constantinou PE, Diehl MR. 2010 Two kinesins transport cargo primarily via the action of one motor: implications for intracellular transport. *Biophys. J.* **99**, 2967–2977. (doi:10.1016/j.bpj.2010.08.025)
- Linari M, Dobbie I, Reconditi M, Koubassova N, Irving M, Piazzesi G, Lombardi V. 1998 The stiffness of skeletal muscle in isometric contraction and rigor: the fraction of myosin heads bound to actin. *Biophys. J.* **74**, 2459–2473. (doi:10.1016/S0006-3495(98)77954-8)
- Piazzesi G, Reconditi M, Linari M, Lucii L, Sun Y-B, Narayanan T, Boesecke P, Lombardi V, Irving M. 2002 Mechanisms of force generation by myosin heads in skeletal muscle. *Nature* **415**, 659–662. (doi:10.1038/415659a)
- Piazzesi G *et al.* 2007 Skeletal muscle performance determined by modulation of number of myosin motors rather than motor force or stroke. *Cell* **131**, 784–795. (doi:10.1016/j.cell.2007.09.045)
- Finer JT, Simmons RM, Spudich JA. 1994 Single myosin molecule mechanics: piconewton forces



- and nanometre steps. *Nature* **368**, 113–119. (doi:10.1038/368113a0)
50. Ishijima A, Harada Y, Kojima H, Funatsu T, Higuchi H, Yanagida T. 1994 Single-molecule analysis of the actomyosin motor using nano-manipulation. *Biochem. Biophys. Res. Comm.* **199**, 1057–1063. (doi:10.1006/bbrc.1994.1336)
  51. Miyata H, Yoshikawa H, Hakozaki H, Suzuki N, Furuno T, Ikegami A, Kinoshita, Jr K, Nishizaka T, Ishiwata S. 1995 Mechanical measurements of single actomyosin motor force. *Biophys. J.* **68**, 2865–2905.
  52. Tsaturyan AK, Bershteyn SY, Koubassova NA, Fernandez M, Narayanan T, Ferenczi MA. 2011 The fraction of myosin motors that participate in isometric contraction of rabbit muscle fibers at near-physiological temperature. *Biophys. J.* **101**, 404–410. (doi:10.1016/j.bpj.2011.06.008)
  53. Nishizaka T, Miyata H, Yoshikawa H, Ishiwata S, Kinoshita, Jr K. 1995 Mechanical properties of single protein motor of muscle studied by optical tweezers. *Biophys. J.* **68**, 755.
  54. Nishizaka T, Miyata H, Yoshikawa H, Ishiwata S, Kinoshita, Jr K. 1995 Unbinding force of a single motor molecule of muscle measured using optical tweezers. *Nature* **377**, 251–254. (doi:10.1038/377251a0)
  55. Takagi Y, Homsher EE, Goldman YE, Shuman H. 2006 Force generation in single conventional actomyosin complexes under high dynamic load. *Biophys. J.* **90**, 1295–1307. (doi:10.1529/biophysj.105.068429)
  56. Moriyama Y, Yasuda K, Ishiwata S, Asai H. 1996  $Ca^{2+}$ -induced tension development in the stalks of glycerinated *Vorticella convallaria*. *Cell Motil. Cytoskeleton* **34**, 271–278. (doi:10.1002/(SICI)1097-0169(1996)34:4<271::AID-CM2>3.0.CO;2-B)
  57. Ryu S, Lang MJ, Matsudaira P. 2012 Maximal force characteristics of the  $Ca^{2+}$ -powered actuator of *Vorticella convallaria*. *Biophys. J.* **103**, 860–867. (doi:10.1016/j.bpj.2012.07.038)
  58. Jass J, Schedin S, Fällman E, Ohlsson J, Nilsson UJ, Uhlén BE, Axner O. 2004 Physical properties of *Escherichia coli* P Pili measured by optical tweezers. *Biophys. J.* **87**, 4271–4283. (doi:10.1529/biophysj.104.044867)
  59. Fällman E, Schedin S, Jass J, Uhlén B-E, Axner O. 2005 The unfolding of the P pili quaternary structure by stretching is reversible, not plastic. *EMBO Rep.* **6**, 52–56. (doi:10.1038/sj.embor.7400310)
  60. Andersson M, Fällman E, Uhlén BE, Axner O. 2006 Dynamic force spectroscopy of *E. coli* P pili. *Biophys. J.* **91**, 2717–2725. (doi:10.1529/biophysj.106.087429)
  61. Kaiser D. 2000 Bacterial motility: how do pili pull? *Curr. Biol.* **10**, R777–R780. (doi:10.1016/S0960-9822(00)00764-8)
  62. Merz AJ, So M, Sheetz MP. 2000 Pilus retraction powers bacterial twitching motility. *Nature* **407**, 98–102. (doi:10.1038/35024105)
  63. Noji H, Yasuda R, Yoshida M, Kinoshita, Jr K. 1997 Direct observation of the rotation of F1-ATPase. *Nature* **386**, 299–302. (doi:10.1038/386299a0)
  64. Berry RM, Berg HC. 1997 Absence of a barrier to backwards rotation of the bacterial flagellar motor demonstrated with optical tweezers. *Proc. Natl Acad. Sci. USA* **94**, 14 433–14 437. (doi:10.1073/pnas.94.26.14433)
  65. Berg HC. 1995 Torque generation by the flagellar rotary motor. *Biophys. J.* **68**, 1635–1675.
  66. Sowa Y, Hotta H, Homma M, Ishijima A. 2003 Torque–speed relationship of the  $Na^{+}$ -driven flagellar motor of *Vibrio alginolyticus*. *J. Mol. Biol.* **327**, 1043–1051. (doi:10.1016/S0022-2836(03)00176-1)
  67. Nakamura S, Kami-Ike N, Yokota J-IP, Kudo S, Minamoto T, Namba K. 2009 Effect of intracellular pH on the torque–speed relationship of bacterial proton-driven flagellar motor. *J. Mol. Biol.* **386**, 332–338. (doi:10.1016/j.jmb.2008.12.034)
  68. Lowe G, Meister M, Berg HC. 1987 Rapid rotation of flagellar bundles in swimming bacteria. *Nature* **325**, 637–640. (doi:10.1038/325637a0)
  69. Powers K, Schappacher-Tilp G, Jinha A, Leonard T, Nishikawa K, Herzog W. 2014 Titin force is enhanced in actively stretched skeletal muscle. *J. Exp. Biol.* **217**, 3629–3636. (doi:10.1242/jeb.105361)
  70. Telley IA, Denoth J, Stüssi E, Pfitzer G, Stehle R. 2006 Half-sarcomere dynamics in myofibrils during activation and relaxation studied by tracking fluorescent markers. *Biophys. J.* **90**, 514–530. (doi:10.1529/biophysj.105.070334)
  71. Shimamoto Y, Kono F, Suzuki M, Ishiwata S. 2007 Nonlinear force-length relationship in the ADP-induced contraction of skeletal myofibrils. *Biophys. J.* **93**, 4330–4341. (doi:10.1529/biophysj.107.110650)
  72. Colomo F, Piroddi N, Poggesi C, te Kronnie G, Tesi C. 1997 Active and passive forces of isolated myofibrils from cardiac and fast skeletal muscle of the frog. *J. Physiol.* **500**, 535–548. (doi:10.1113/jphysiol.1997.sp022039)
  73. Brandt PW, Colomo F, Piroddi N, Poggesi C, Tesi C. 1998 Force regulation by  $Ca^{2+}$  in skinned single cardiac myocytes of frog. *Biophys. J.* **74**, 1994–2004. (doi:10.1016/S0006-3495(98)77906-8)
  74. Krüger M, Zittich S, Redwood C, Blaudeck N, James J, Robbins J, Pfitzer G, Stehle R. 2005 Effects of the mutation R145G in human cardiac troponin I on the kinetics of the contraction–relaxation cycle in isolated cardiac myofibrils. *J. Physiol. (Lond.)* **564**, 347–357. (doi:10.1113/jphysiol.2004.079095)
  75. Stehle R, Krüger M, Pfitzer G. (2002) Force kinetics and individual sarcomere dynamics in cardiac myofibrils after rapid  $Ca^{2+}$  changes. *Biophys. J.* **83**, 2152–2161. (doi:10.1016/S0006-3495(02)73975-1)
  76. Stehle R, Krüger M, Scherer P, Brixius K, Schwinger RHG, Pfitzer G. (2002) Isometric force kinetics upon rapid activation and relaxation of mouse, guinea pig and human heart muscle studied on the subcellular myofibrillar level. *Basic Res. Cardiol.* **97**(Suppl. 1), I/127–I/135.
  77. Stehle R, Solzin J, Iorga B, Gomez D, Blaudeck N, Pfitzer G. 2006 Mechanical properties of sarcomeres during cardiac myofibrillar relaxation: stretch-induced cross-bridge detachment contributes to early diastolic filling. *J. Muscle Res. Cell Motil.* **27**, 423–434. (doi:10.1007/s10974-006-9072-7)
  78. Linke WA, Popov V, Pollack GH. 1994 Passive and active tension in single cardiac myofibrils. *Biophys. J.* **67**, 782–792. (doi:10.1016/S0006-3495(94)80538-7)
  79. Wang Q, Newhard CS, Ramanath S, Sheppard D, Swank DM. 2014 An embryonic myosin converter domain influences *Drosophila* indirect flight muscle stretch activation, power generation and flight. *J. Exp. Biol.* **217**, 290–298. (doi:10.1242/jeb.091769)
  80. Holmes JM, Hilber K, Galler S, Neil DM. 1999 Shortening properties of two biochemically defined muscle fibre types of the Norway lobster *Nephrops norvegicus* L. *J. Muscle Res. Cell Motil.* **20**, 265–278. (doi:10.1023/A:1005481725344)
  81. Tameyasu T. 1992 Unloaded shortening after a quick release of a contracting, single fibre from crayfish slow muscle. *J. Muscle Res. Cell Motil.* **13**, 619–629. (doi:10.1007/BF01738251)
  82. Gilmour KM, Ellington CP. 1993 Power output of glycerinated bumblebee flight muscle. *J. Exp. Biol.* **183**, 77–100.
  83. Johnston IA, Brill R. 1984 Thermal dependence of contractile properties of single skinned muscle fibres from Antarctic and various warm water marine fishes including skipjack tuna (*Katsuwonus pelamis*) and Kawakawa (*Euthynnus affinis*). *J. Comp. Physiol. B* **155**, 63–70. (doi:10.1007/BF00688792)
  84. Johnston IA, Altringham JD. 1985 Evolutionary adaptation of muscle power output to environmental temperature: force-velocity characteristics of skinned fibres isolated from antarctic, temperate and tropical marine fish. *Pflügers Arch. Eur. J. Physiol.* **405**, 136–140. (doi:10.1007/BF00584534)
  85. Altringham JD, Johnston IA. 1982 The pCa-tension and force-velocity characteristics of skinned fibres isolated from fish fast and slow muscles. *J. Physiol. Lond.* **333**, 421–449. (doi:10.1113/jphysiol.1982.sp014462)
  86. Johnston IA, Salamonski J. 1984 Power output and force-velocity relationship of red and white muscle fibres from the pacific blue marlin (*Makaira nigricans*). *J. Exp. Biol.* **111**, 171–177.
  87. Wakeling JM, Johnston IA. 1998 Muscle power output limits fast-start performance in fish. *J. Exp. Biol.* **201**, 1505–1526.
  88. Lännergren J. 1978 The force-velocity relation of isolated twitch and slow muscle fibres of *Xenopus laevis*. *J. Physiol. (Lond.)* **283**, 501–521. (doi:10.1113/jphysiol.1978.sp012516)
  89. Lännergren J. 1992 Fibre types in *Xenopus* muscle and their functional properties. In *Muscular contraction* (ed. RM Simmons), pp. 181–188. London, UK: Cambridge University Press.
  90. Mutungi G, Johnston IA. 1987 The effects of temperature and pH on the contractile properties of skinned muscle fibres from the terrapin, *Pseudemys scripta elegans*. *J. Exp. Biol.* **128**, 87–105. (doi:10.1113/jphysiol.1996.sp021403)
  91. Reiser PJ, Welch Jr KC, Suarez RK, Altschuler DL. 2013 Very low force-generating ability and unusually high temperature dependency in hummingbird flight muscle fibers. *J. Exp. Biol.* **216**, 2247–2256. (doi:10.1242/jeb.068825)
  92. Reiser PJ, Greaser ML, Moss RL. 1996 Contractile properties and protein isoforms of single fibres from the chicken pectoralis red strip muscle. *J. Physiol. (Lond.)* **493**, 553–562. (doi:10.1113/jphysiol.1996.sp021403)
  93. West TG, Toepfer CN, Wolegede RC, Curtin NA, Rowlerson A, Kalakoutis M, Hudson P, Wilson AM. 2013 Power output of skinned skeletal muscle fibres from the cheetah (*Acinonyx jubatus*). *J. Exp. Biol.* **216**, 2974–2982. (doi:10.1242/jeb.083667)

94. Seow CY, Ford LE. 1991 Shortening velocity and power output of skinned muscle fibers from mammals having a 25 000-fold range of body mass. *J. Gen. Physiol.* **97**, 541–560. (doi:10.1085/jgp.97.3.541)
95. Kohn TA, Noakes TC. 2013 Lion (*Panthera leo*) and caracal (*Caracal caracal*) type IIX single muscle fibre force and power exceed that of trained humans. *J. Exp. Biol.* **216**, 960–969. (doi:10.1242/jeb.078485)
96. Rome LC, Sosnicki AA, Goble DO. 1990 Maximum velocity of shortening of three fibre types from horse soleus muscle: implications for scaling with body size. *J. Physiol. (Lond.)* **431**, 173–185. (doi:10.1113/jphysiol.1990.sp018325)
97. Bottinelli R, Canepari M, Pellegrino MA, Reggiani C. 1996 Force-velocity properties of human skeletal muscle fibres: myosin heavy chain isoform and temperature dependence. *J. Physiol. (Lond.)* **495**, 573–586. (doi:10.1113/jphysiol.1996.sp021617)
98. Larsson L, Moss RL. 1993 Maximum velocity of shortening in relation to myosin isoform composition in single fibres from human skeletal muscles. *J. Physiol. (Lond.)* **472**, 595–614. (doi:10.1113/jphysiol.1993.sp019964)
99. Fitts RH, Desplanches D, Romatowski JG, Widrick JJ. 2000 Spaceflight effects on single skeletal muscle fiber function in the rhesus monkey. *Am. J. Physiol. Regul. Integr. Comp. Physiol.* **279**, R1546–R1557.
100. Pellegrino MA, Canepari M, Rossi R, D'Antona G, Reggiani C, Bottinelli R. 2003 Orthologous myosin isoforms and scaling of shortening velocity with body size in mouse, rat, rabbit and human muscles. *J. Physiol. (Lond.)* **546**, 677–689. (doi:10.1113/jphysiol.2002.027375)
101. Sweeney HL, Kushmerick MJ, Mabucid K, Gergely J, Sreter FA. 1986 Velocity of shortening and myosin isoenzymes in two types of rabbit fast-twitch muscles. *Am. J. Physiol.* **251**, C431–C484.
102. Schiaffino S, Reggiani C. 1996 Molecular diversity of myofibrillar proteins: gene regulation and functional significance. *Physiol. Rev.* **76**, 371–423.
103. Sweeney HL, Kushmerick MJ, Mabuchi K, Sreter FA, Gergely J. 1988 Myosin alkali light chain and heavy chain variations correlate with altered shortening velocity of isolated skeletal muscle fibers. *J. Biol. Chem.* **263**, 9034–9039.
104. Greaser ML, Moss RL, Reiser PJ. 1988 Variations in contractile properties of rabbit single muscle fibres in relation to troponin T isoforms and myosin light chains. *J. Physiol. (Lond.)* **406**, 85–98. (doi:10.1113/jphysiol.1988.sp017370)
105. Bottinelli R, Canepari M, Reggiani C, Stienen GJM. 1994 Myofibrillar ATPase activity during isometric contraction and isomyosin composition in rat single skinned muscle fibres. *J. Physiol. (Lond.)* **481**, 663–675. (doi:10.1113/jphysiol.1994.sp020472)
106. Sexton AW, Gersten JW. 1967 Isometric tension differences in fibers of red and white muscles. *Science* **157**, 199. (doi:10.1126/science.157.3785.199)
107. Sexton AW. 1967 Isometric tension of glycerinated muscle fibers following adrenalectomy. *Am. J. Physiol.* **212**, 313–316.
108. Eddinger TJ, Moss RL. 1987 Mechanical properties of skinned single fibers of identified types from rat diaphragm. *Am. J. Physiol.* **253**, C210–C218.
109. Milligan BJ, Curtin NA, Bone Q. 1997 Contractile properties of obliquely striated muscle from the mantle of squid (*Alloteuthis subulata*) and cuttlefish (*Sepia officinalis*). *J. Exp. Biol.* **200**, 2425–2436.
110. Olson JM, Marsh RL. 1998 Activation patterns and length changes in hindlimb muscles of the bullfrog *Rana catesbeiana* during jumping. *J. Exp. Biol.* **201**, 2763–2777.
111. Stokes DR, Josephson RK. 1994 Contractile properties of a high-frequency muscle from a crustacean. II. Contraction kinetics. *J. Exp. Biol.* **187**, 275–293.
112. Jahromi SS, Atwood HL. 1969 Correlation of structure, speed of contraction, and total tension in fast and slow abdominal muscle fibers of the lobster (*Homarus americanus*). *J. Exp. Zool.* **171**, 25–38. (doi:10.1002/jez.1401710105)
113. Elnor RW, Campbell A. 1981 Force, function and mechanical advantage in the chelae of the American lobster *Homarus americanus* (Decapoda: Crustacea). *J. Zool. Lond.* **193**, 269–286. (doi:10.1111/j.1469-7998.1981.tb03444.x)
114. Josephson RK, Ellington CP. 1997 Power output from a flight muscle of the bumblebee *Bombus terrestris*. I. Some features of the dorso-ventral flight muscle. *J. Exp. Biol.* **200**, 1215–1226.
115. Josephson RK, Malamud JG, Stokes DR. 2000 Power output by an asynchronous flight muscle from a beetle. *J. Exp. Biol.* **203**, 2667–2689.
116. Fitzhugh GH, Marden JH. 1997 Maturational changes in troponin T expression, Ca<sup>2+</sup>-sensitivity and twitch contraction kinetics in dragonfly flight muscle. *J. Exp. Biol.* **200**, 1473–1482.
117. Marden JH. 1995 Evolutionary adaptation of contractile performance in muscle of ectothermic winter-flying moths. *J. Exp. Biol.* **198**, 2087–2094.
118. Josephson RK. 1984 Contraction dynamics of flight and stridulatory muscles of Tettigoniid insects. *J. Exp. Biol.* **108**, 77–96.
119. Malamud JG, Josephson RK. 1991 Force-velocity relationships of a locust flight muscle at different times during a twitch contraction. *J. Exp. Biol.* **159**, 65–87.
120. Granzier HLM, Wiersma J, Akster HA, Osse JWM. 1983 Contractile properties of a white- and a red-fibre type of the M. hyohyoideus of the carp (*Cyprinus carpio* L.). *J. Comp. Physiol. B* **149**, 441–449. (doi:10.1007/BF00690001)
121. Rome LC, Sosnicki AA. 1990 The influence of temperature on mechanics of red muscle in carp. *J. Physiol. Lond.* **427**, 151–169. (doi:10.1113/jphysiol.1990.sp018165)
122. James RS, Cole NJ, Davies MLF, Johnston IA. 1998 Scaling of intrinsic contractile properties and myofibrillar protein composition of fast muscles in the fish *Myoxocephalus scorpius* L. *J. Exp. Biol.* **201**, 901–912.
123. Franklin CE, Johnston IA. 1997 Muscle power output during escape responses in an Antarctic fish. *J. Exp. Biol.* **200**, 703–712.
124. Curtin NA, Woledge RC. 1988 Power output and force-velocity relationship of live fibres from white myotomal muscle of the dogfish, *Scyliorhinus canicula*. *J. Exp. Biol.* **140**, 187–197.
125. Lou F, Curtin NA, Woledge RC. 1997 The energetic cost of activation of white muscle fibres from the dogfish *Scyliorhinus canicula*. *J. Exp. Biol.* **200**, 495–501.
126. Coughlin DJ, Zhang G, Rome LC. 1996 Contraction dynamics and power production of pink muscle of the scup (*Stenotomus chrysops*). *J. Exp. Biol.* **199**, 2703–2712.
127. Else PL, Bennet AF. 1987 The thermal dependence of locomotor performance and muscle contractile function in the salamander *Ambystoma tigrinum nebulosum*. *J. Exp. Biol.* **128**, 219–233.
128. Johnston IA, Gleeson TT. 1987 Effects of temperature on contractile properties of skinned muscle fibers from three toad species. *Am. J. Physiol. (Regul. Integr. Comp. Physiol.)* **252**, R371–R375.
129. McLister JD, Stevens ED, Bogart JP. 1995 Comparative contractile dynamics of calling and locomotor muscles in three hylid frogs. *J. Exp. Biol.* **198**, 1527–1538.
130. Peplowski MM, Marsh RL. 1997 Work and power output in the hindlimb muscles of Cuban tree frogs *Osteopilus septentrionalis* during jumping. *J. Exp. Biol.* **200**, 2861–2870.
131. Peters SE, Aulner DA. 2000 Sexual dimorphism in forelimb muscles of the bullfrog, *Rana catesbeiana*: a functional analysis of isometric contractile properties. *J. Exp. Biol.* **203**, 3639–3654.
132. Stienen GJM, Blangé T, Schnerr MC. 1978 Tension responses of frog sartorius muscle to quick ramp-shaped shortenings and some effects of metabolic inhibition. *Pflügers Arch.* **376**, 97–104. (doi:10.1007/BF00581573)
133. Lutz GJ, Rome LC. 1996 Muscle function during jumping in frogs. II. Mechanical properties of muscle: implications for system design. *Am. J. Physiol. Cell Physiol.* **271**, C571–C578.
134. Seebacher F, Tallis JA, James RS. 2014 The cost of muscle power production: muscle oxygen consumption per unit work increases at low temperatures in *Xenopus laevis*. *J. Exp. Biol.* **217**, 1940–1945. (doi:10.1242/jeb.101147)
135. Marsh RL. 1988 Ontogenesis of contractile properties of skeletal muscle and sprint performance in the lizard *Dipsosaurus dorsalis*. *J. Exp. Biol.* **137**, 119–139.
136. Marsh RL, Bennet AF. 1986 Thermal dependence of contractile properties of skeletal muscle from the lizard *Sceloporus occidentalis* with comments of methods for fitting and comparing force-velocity curves. *J. Exp. Biol.* **126**, 63–77.
137. Askew GN, Marsh RL. 2001 The mechanical power output of the pectoralis muscle of the blue-breasted quail (*Coturnix chinensis*): the *in vivo* length cycle and its implications for muscle performance. *J. Exp. Biol.* **204**, 3587–3600.
138. Asmussen G, Maréchal G. 1989 Maximal shortening velocities, isomyosins and fibre types in soleus muscle of mice, rats, and guinea-pigs. *J. Physiol. (Lond.)* **416**, 245–254. (doi:10.1113/jphysiol.1989.sp017758)
139. Perry AK, Blickhan R, Biewener AA, Heglund NC, Taylor CR. 1988 Preferred speeds in terrestrial vertebrates: are they equivalent? *J. Exp. Biol.* **137**, 207–219.
140. Biewener AA, Blickhan R, Perry AK, Heglund NC, Taylor CR. 1988 Muscle forces during locomotion in kangaroo rats: force platform and tendon buckle measurements compared. *J. Exp. Biol.* **137**, 191–205.

141. Ettema GJC. 1996 Elastic and length-force characteristics of the gastrocnemius of the hopping mouse (*Notomys alexis*) and the rat (*Rattus norvegicus*). *J. Exp. Biol.* **199**, 1277–1285.
142. Burke RE, Tsairis P. 1973 Anatomy and innervation ratios in motor units of cat gastrocnemius. *J. Physiol. (Lond.)* **234**, 749–765. (doi:10.1113/jphysiol.1973.sp010370)
143. Choi I, Cho Y, Oh IK, Jung N, Shin H. 1998 Behavior and muscle performance in heterothermic bats. *Physiol. Zool.* **71**, 257–266. (doi:10.1086/515915)
144. Rowe RWD. 1969 The effect of hypertrophy on the properties of skeletal muscle. *Comp. Biochem. Physiol.* **28**, 1449–1453. (doi:10.1016/0010-406X(69)90583-0)
145. Luff AR. 1981 Dynamic properties of the inferior rectus, extensor digitorum longus, diaphragm and soleus muscles of the mouse. *J. Physiol. (Lond.)* **313**, 161–171. (doi:10.1113/jphysiol.1981.sp013656)
146. Barclay CJ, Constable JK, Gibbs CL. 1993 Energetics of fast- and slow-twitch muscles of the mouse. *J. Physiol. (Lond.)* **472**, 61–80. (doi:10.1113/jphysiol.1993.sp019937)
147. Askew GN, Marsh RL. 1997 The effects of length trajectory on the mechanical power output of mouse skeletal muscles. *J. Exp. Biol.* **200**, 3119–3131.
148. Asmussen G, Beckers-Bleuix G, Maréchal G. 1994 The force-velocity relation of the rabbit inferior oblique muscle: influence of temperature. *Pflügers Arch. Eur. J. Physiol.* **426**, 542–547. (doi:10.1007/BF00378532)
149. Kanda K, Hashizume K. 1992 Factors causing difference in force output among motor units in the rat medial gastrocnemius muscle. *J. Physiol. (Lond.)* **448**, 677–695. (doi:10.1113/jphysiol.1992.sp019064)
150. Close R. 1969 Dynamic properties of fast and slow skeletal muscles of the rat after nerve cross-union. *J. Physiol. Lond.* **204**, 331–346. (doi:10.1113/jphysiol.1969.sp008916)
151. Bárány M, Close RI. 1971 The transformation of myosin in cross-innervated rat muscles. *J. Physiol. (Lond.)* **213**, 455–474. (doi:10.1113/jphysiol.1971.sp009393)
152. Ranatunga KW. 1982 Temperature-dependence of shortening velocity and rate of isometric tension development in rat skeletal muscle. *J. Physiol. (Lond.)* **329**, 465–483. (doi:10.1113/jphysiol.1982.sp014314)
153. Goffart M, Ritchie JM. 1952 The effect of adrenaline on the contraction of mammalian skeletal muscle. *J. Physiol. (Lond.)* **116**, 357–371. (doi:10.1113/jphysiol.1952.sp004710)
154. Johnson B, Wilson LE, Zhan WZ, Watchko JF, Daoud MJ, Sieck GC. 1994 Contractile properties of the developing diaphragm correlate with myosin heavy chain phenotype. *J. Appl. Physiol.* **77**, 481–487.
155. Morgan DL, Proske U, Warren D. 1978 Measurements of muscle stiffness and the mechanism of elastic storage of energy in hopping kangaroos. *J. Physiol. (Lond.)* **282**, 253–261. (doi:10.1113/jphysiol.1978.sp012461)
156. Govind CK, Blundon JA. 1985 Form and function of the asymmetric chela in blue crabs with normal and reversed handedness. *Biol. Bull.* **168**, 321–331. (doi:10.2307/1541244)
157. Taylor GM. 2000 Maximum force production: why are crabs so strong? *Proc. R. Soc. Lond. B* **267**, 1475–1480. (doi:10.1098/rspb.2000.1167)
158. Blundon JA. 1988 Morphology and muscle stress of chelae of temperate and tropical stone crabs *Menippe mercenaria*. *J. Zool. Lond.* **215**, 663–673. (doi:10.1111/j.1469-7998.1988.tb02402.x)
159. Heethoff M, Koerner L. 2007 Small but powerful: the oribatid mite *Archegozetes longisetosus* Aoki (Acari, Oribatida) produces disproportionately high forces. *J. Exp. Biol.* **210**, 3036–3042. (doi:10.1242/jeb.008276)
160. Evans MEG. 1973 The jump of the click beetle (Coleoptera: Elateridae): energetics and mechanics. *J. Zool. Lond.* **169**, 181–194. (doi:10.1111/j.1469-7998.1973.tb04553.x)
161. Evans MEG. 1977 Locomotion in the Coleoptera Adephaga, especially Carabidae. *J. Zool. Lond.* **181**, 189–226.
162. Goyens J, Dirck J, Dierick M, Van Hoorebeke L, Aerts P. 2014 Biomechanical determinants of bite force dimorphism in *Cyclommatus metallifer* stag beetles. *J. Exp. Biol.* **217**, 1065–1071. (doi:10.1242/jeb.091744)
163. Dickinson MH, Lighton JRB. 1995 Muscle efficiency and elastic storage in the flight motor of *Drosophila*. *Science* **268**, 87–90. (doi:10.1126/science.7701346)
164. Bennet-Clark HC. 1975 The energetics of the jump of the locust *Schistocerca gregaria*. *J. Exp. Biol.* **63**, 53–83.
165. Bennet-Clark HC, Lucey ECA. 1967 The jump of the flea: a study of the energetics and a model of the mechanism. *J. Exp. Biol.* **47**, 59–76.
166. Biewener AA. 2005 Biomechanical consequences of scaling. *J. Exp. Biol.* **208**, 1665–1676. (doi:10.1242/jeb.01520)
167. Biewener AA, Corning WR. 2001 Dynamics of mallard (*Anas platyrhynchos*) gastrocnemius function during swimming versus terrestrial locomotion. *J. Exp. Biol.* **204**, 1745–1756.
168. Williamson MR, Dial KP, Biewener AA. 2001 Pectoralis muscle performance during ascending and slow level flight in mallards (*Anas platyrhynchos*). *J. Exp. Biol.* **204**, 495–507. (doi:10.1242/jeb.043497)
169. Dial KP, Biewener AA. 1993 Pectoralis muscle force and power output during different modes of flight in pigeons (*Columba livia*). *J. Exp. Biol.* **176**, 31–54.
170. Daley MA, Biewener AA. 2003 Muscle force-length dynamics during level versus incline locomotion: a comparison of *in vivo* performance of two guinea fowl ankle extensors. *J. Exp. Biol.* **206**, 2941–2958. (doi:10.1242/jeb.00503)
171. Biewener AA, Dial KP, Goslow GE. 1992 Pectoralis muscle force and power output during flight in the starling. *J. Exp. Biol.* **164**, 1–18. (doi:10.1016/0022-0981(92)90132-T)
172. Alexander RM. 1974 The mechanics of jumping by a dog (*Canis familiaris*). *J. Zool. Lond.* **173**, 549–573. (doi:10.1111/j.1469-7998.1974.tb04134.x)
173. Jayes AS, Alexander RM. 1982 Estimates of mechanical stresses in leg muscles of galloping greyhounds (*Canis familiaris*). *J. Zool. Lond.* **198**, 315–328. (doi:10.1111/j.1469-7998.1982.tb02078.x)
174. Biewener AA, Blickhan R. 1988 Kangaroo rat locomotion: design for elastic energy storage or acceleration? *J. Exp. Biol.* **140**, 243–255.
175. Biewener AA. 1998 Muscle-tendon stresses and elastic energy storage during locomotion in the horse. *Comp. Biochem. Physiol. B* **120**, 73–87. (doi:10.1016/S0305-0491(98)00024-8)
176. Herzog W, Leonard TR, Guimaraes ACS. 1993 Forces in gastrocnemius, soleus and plantaris muscles for the freely moving cat. *J. Biomech.* **26**, 945–953. (doi:10.1016/0021-9290(93)90056-K)
177. Thorpe SKS, Li Y, Crompton RH, Alexander RM. 1998 Stresses in human leg muscles in running and jumping determined by force plate analysis and from published magnetic resonance images. *J. Exp. Biol.* **201**, 63–70.
178. Rutherford OM, Jones DA. 1992 Measurement of fibre pennation using ultrasound in the human quadriceps *in vivo*. *Eur. J. Appl. Physiol.* **65**, 433–437. (doi:10.1007/BF00243510)
179. Reeves ND, Narici MV, Maganaris CN. 2004 Effect of resistance training on skeletal muscle-specific force in elderly humans. *J. Appl. Physiol.* **96**, 885–892. (doi:10.1152/jappphysiol.00688.2003)
180. O'Brien TD, Reeves ND, Baltzopoulos V, Jones DA, Maganaris CN. 2009 *In vivo* measurements of muscle specific tension in adults and children. *Exp. Physiol.* **95**, 202–210. (doi:10.1113/expphysiol.2009.048967)
181. Kanehisa H, Ikegawa S, Fukunaga T. 1994 Comparison of muscle cross-sectional area and strength between untrained women and men. *Eur. J. Appl. Physiol.* **68**, 148–154. (doi:10.1007/BF00244028)
182. Maganaris CN, Baltzopoulos V, Ball D, Sargeant AJ. 2001 *In vivo* specific tension of human skeletal muscle. *J. Appl. Physiol.* **90**, 865–872.
183. Narici MV, Landoni L, Minetti AE. 1992 Assessment of human knee extensor muscles stress from *in vivo* physiological cross-sectional area and strength measurements. *Eur. J. Appl. Physiol.* **65**, 438–444. (doi:10.1007/BF00243511)
184. Erskine RM, Jones DA, Maganaris CN, Degens H. 2009 *In vivo* specific tension of the human quadriceps femoris muscle. *Eur. J. Appl. Physiol.* **106**, 827–838. (doi:10.1007/s00421-009-1085-7)
185. Davies CTM, Thomas DO, White MJ. 1986 Mechanical properties of young and elderly human muscle. *Acta Med. Scand. Suppl.* **711**, 219–226.
186. Fukunaga T, Roy RR, Shellock FG, Hodgson JA, Edgerton VR. 1996 Specific tension of human plantar flexors and dorsiflexors. *J. Appl. Physiol.* **80**, 158–165.
187. Haxton HA. 1944 Absolute muscle force in the ankle flexors of man. *J. Physiol. (Lond.)* **103**, 267–273. (doi:10.1113/jphysiol.1944.sp004075)
188. Hermann L. 1898 Zur messung der muskelfraft am menschen. *Pflügers Arch.* **73**, 429–437. (doi:10.1007/BF01795980)
189. Reys JHO. 1915 Über die absolute muskelfraft in menschlichen körper. *Pflügers Arch.* **160**, 133–204. (doi:10.1007/BF01680963)
190. Weber E. 1846 *Handwörterbuch der Physiologie mit Rücksicht auf physiologische Pathologie*. Braunschweig, Germany: Verlag.
191. Alexander RM, Maloiy GMD, Hunter B, Jayes AS, Nturiubi J. 1979 Mechanical stresses in fast locomotion of buffalo (*Syncerus caffer*) and elephant (*Loxodonta africana*). *J. Zool. Lond.* **189**, 135–144. (doi:10.1111/j.1469-7998.1979.tb03956.x)

192. Biewener AA, Baudinette RV. 1995 *In vivo* muscle force and elastic energy storage during steady-speed hopping of tammar wallabies (*Macropus eugenii*). *J. Exp. Biol.* **198**, 1829–1841.
193. Alexander RM, Vernon A. 1975 The mechanics of hopping by kangaroos (Macropodidae). *J. Zool. Lond.* **177**, 265–303. (doi:10.1111/j.1469-7998.1975.tb05983.x)
194. Siegel S. 1956 *Nonparametric statistics for the behavioral sciences*. New York, NY: McGraw-Hill.
195. Brocchieri L, Karlin S. 2005 Protein length in eukaryotic and prokaryotic proteomes. *Nucleic Acids Res.* **33**, 3390–3400. (doi:10.1093/nar/gki615)
196. Erickson HP. 2009 Size and shape of protein molecules at the nanometer level determined by sedimentation, gel filtration, and electron microscopy. *Biol. Proced. Online* **11**, 32–51. (doi:10.1007/s12575-009-9008-x)
197. Fisher ME, Kolomeisky AB. 1999 Molecular motors and the forces they exert. *Phys. A* **274**, 241–266. (doi:10.1016/S0378-4371(99)00389-1)
198. Bustamante C, Keller D, Oster G. 2001 The physics of molecular motors. *Acc. Chem. Res.* **34**, 412–420. (doi:10.1021/ar0001719)
199. Hess H, Bachand GD, Vogel V. 2004 Powering nanodevices with biomolecular motors. *Chem. Eur. J.* **10**, 2110–2116. (doi:10.1002/chem.200305712)
200. Bao G, Suresh S. 2003 Cell and molecular mechanics of biological materials. *Nat. Mater.* **2**, 715–725. (doi:10.1038/nmat1001)
201. Schliwa M, Woehlke G. 2003 Molecular motors. *Nature* **422**, 759–765. (doi:10.1038/nature01601)
202. Berry J-L, Pelicia V. 2015 Exceptionally widespread nanomachines composed of type IV pili: the prokaryotic Swiss army knives. *FEMS Microbiol. Rev.* **39**, 134–154. (doi:10.1093/femsre/fuu001)
203. Alegre-Cebollada J, Badilla CL, Fernandez JM. 2010 Isopeptide bonds block the mechanical extension of pili in pathogenic *Streptococcus pyogenes*. *J. Biol. Chem.* **285**, 11 235–11 242. (doi:10.1074/jbc.M110.102962)
204. Huxley HE. 1985 The crossbridge mechanism of muscular contraction and its implications. *J. Exp. Biol.* **115**, 17–30.
205. Batters C, Veigel C, Homsher E, Sellers JR. 2014 To understand muscle you must take it apart. *Front. Physiol.* **5**, 1–14. (doi:10.3389/fphys.2014.00090)
206. Lindstedt SL, McGlothlin T, Percy E, Pifer J. 1998 Task-specific design of skeletal muscle: balancing muscle structural composition. *Comp. Biochem. Physiol. B* **120**, 35–40. (doi:10.1016/S0305-0491(98)00021-2)
207. Gordon AM, Huxley AF, Julian FJ. 1966 The variation in isometric tension with sarcomere length in vertebrate muscle fibres. *J. Physiol. (Lond.)* **184**, 170–192. (doi:10.1113/jphysiol.1966.sp007909)
208. Josephson RK. 1975 Extensive and intensive factors determining the performance of striated muscle. *J. Exp. Zool.* **194**, 135–153. (doi:10.1002/jez.1401940109)
209. Otten E. 1987 Optimal design of vertebrate and insect sarcomeres. *J. Morphol.* **191**, 49–62. (doi:10.1002/jmor.1051910106)
210. Gokhin DS, Kim EN, Lewis SA, Hoenecke HR, D'Lima DD, Fowler VM. 2012 Thin-filament length correlates with fiber type in human skeletal muscle. *Am. J. Physiol. Cell. Physiol.* **302**, C555–C565. (doi:10.1152/ajpcell.00299.2011)
211. Meyer-Vernet N, Rospars J-P. 2015 How fast do living organisms move: maximum speeds from bacteria to elephants and whales. *Am. J. Phys.* **83**, 719–722. (doi:10.1119/1.4917310)